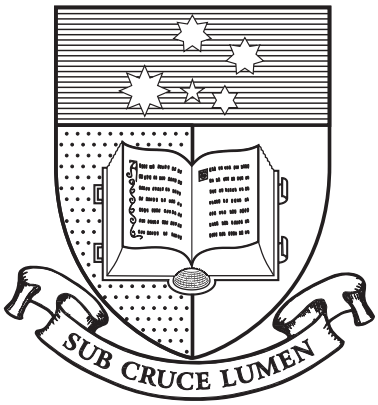

The University of Adelaide

School of Mechanical Engineering

Assessment of the Temporal Release of Atomic Sodium During a Burning Black Liquor Droplet Using Quantitative Planar Laser-Induced Fluorescence (PLIF)

Woei Lean Saw

PhD Thesis

June 2009

Table of Contents

Table of Contents ..... *i*

List of Figures and Table ..... *iii*

Abstract ..... *v*

Preface ..... *vii*

Thesis Declaration ..... *ix*

List of Publications ..... *xi*

Acknowledgements ..... *xiii*

Summary of Each Paper ..... *xv*

Chapter 1. Introduction *1*

Chapter 2. Background *7*

2.1. Black liquor *7*

2.2. Release of sodium during black liquor combustion *9*

2.2.1. Measurement of the release of sodium *10*

2.2.2. Equilibrium and kinetic calculations on the release of sodium *12*

2.3. Autocausticizing *13*

2.3.1. Autocausticizing using sodium borates *14*

2.3.2. Partial autocausticizing using sodium borates *15*

2.3.3. Influence of boron on the release of sodium *16*

2.4. Implementation of laser diagnostics technique on the release of alkali metal from solid fuel *17*

2.4.1 Laser-induced fluorescence (LIF) *17*

2.4.1.1. The implementation of LIF on the release of atomic sodium *18*

2.4.1.2. Limitation of LIF *19*

2.5. Surface temperature 20

References 23

Chapter 3. Assessment of the Release of Atomic Na from a Burning Black Liquor Droplet Using Quantitative PLIF 31

Chapter 4. Simultaneous Measurement of the Surface Temperature and the Release of Atomic Sodium from a Burning Black Liquor Droplet 45

Chapter 5. Influence of Droplet Size on the Release of Atomic Sodium from a Burning Black Liquor Droplet in a Flat Flame 81

Chapter 6. The Influence of Boron on the Emission of Sodium During Burning Black Liquor Combustion Under Oxidative Conditions 115

Chapter 7. Influence of Stoichiometry on the Release of Atomic Sodium from a Burning Black Liquor Droplet in a Flat Flame With and Without Boron 127

Chapter 8. Conclusion 157

List of Figures and Table

Figure	Title	Page
Figure 1.1	The average distribution of world's total energy consumption from 1986 to 2006 [1]	2
Figure 1.2	Schematic diagram of the kraft pulping process	4
Figure 2.1	A schematic diagram of the four stages of black liquor combustion	8
Figure 2.2	Lower furnace equilibrium compositions for normal, "open cycle" liquor as function of temperature. Air-to-fuel ratio = 70% (the fuel corresponds to the black liquor) [54]	13
Figure 2.3	The schematic diagram of the kraft pulping process with borate autocausticizing proposed by Janson	15
Figure 2.4	Example of sodium (D_1) atom energy level diagram.	18
Figure 2.5	The variation of fluorescence trapping with absorption	20

Table	Title	Page
Table 1.1	Typical propositions of the organic and inorganic compounds in black liquor	3

Abstract

The release of sodium during the combustion of black liquor is a significant source of fume formation in a kraft recovery boiler, affecting efficiency in a pulp and paper mill. The fume is deposited on the surface of heat exchanger tubes in the upper furnace, causing fouling and corrosion, especially to the superheaters. This thesis reports on work done to develop improved understanding of fume formation.

The mechanisms of sodium release during each stage of black liquor combustion are influenced by the surface temperature. The addition of boron to the black liquor, which debottlenecks the recausticizing plant by a reduction in lime usage, also influences the characteristics of black liquor combustion, such as combustion time and swelling. Previously, no effective measurement technique has been available to quantify sodium concentration in the plume of a burning black liquor droplet with or without boron, or to record the distribution of surface temperature through the time history of a burning droplet. This thesis reports on the adaptation of two techniques for the measurement of the release of atomic sodium and the temperature history, and their application to investigate several aspects of the release of atomic sodium during combustion of black liquor in a flat flame environment.

The simultaneous employment of a planar laser-induced fluorescence (PLIF) technique with an absorption technique has been adapted to allow quantitative measurement of the release of atomic sodium. The absorption technique has been employed to correct for both fluorescence trapping due to absorption and attenuation by high concentration of the atomic sodium in the plume, and for collisional quenching by the other major gas components present in the flat flame. An independent assessment was performed using kinetic calculations, based on measured total sodium that is residual in a particle obtained at different stages in the combustion process. These independent assessments were used to provide greater insight in to the release process and to cross-check. The

influence of both the initial diameter of the droplet and addition of boron to the black liquor on the temporal release and the release rate of atomic sodium during the combustion have been performed using the present PLIF technique.

The second technique, two-dimensional two-colour optical pyrometry, has been adapted to measure the distribution of surface temperature and the swelling (change in surface area) of a burning black liquor droplet. The influence of surface temperature or the change in the external surface area of the droplet on the release of atomic sodium during the combustion of black liquor has been assessed through concurrent use of both adapted techniques.

The highest concentration of atomic sodium was measured in the final stage of combustion that of smelt coalescence, where it is an order of magnitude greater than in the other stages combined. While the extensive release of atomic sodium at high temperature in this final combustion stage occurs in only a relatively small percentage of droplets in a kraft recovery boiler, the effect could still be significant in fume formation. This is because the extensive release is expected to occur in the very small droplets, predominantly generated by splitting or physical ejection. Small droplets will have a very short combustion time and so could remain in suspension within hot gases for sufficient time for extensive release of sodium. These measurements outcomes can be used to support the future development of sub-models for computational fluid dynamics (CFD) models in order to better understand and optimise fume formation in a kraft recovery boiler.

Preface

"A journey of a thousand miles must begin with a single step."

Lao Tze

The work outlined in this thesis was performed in the Schools of Mechanical Engineering and Chemical Engineering at The University of Adelaide from September 2005 to May 2009. A section of the work was also carried out in the Process Chemistry Centre (PCC), Åbo Akademi in 2006 and 2007. This thesis by publication consists of eight chapters, preceded by short summary of each publication. The first chapter introduces the kraft pulping process and the importance of sodium in the pulping process. The second chapter covers the background for this thesis including black liquor, sodium emission, autocausticizing, laser diagnostic technique and surface temperature measurement technique. This chapter also describes the link between each of the publications. The next five chapters consist of five peer-reviewed journal articles, written jointly with other researchers from the PCC. These chapters present the key findings of the release of atomic sodium from black liquor using a laser diagnostic technique under various conditions, and equilibrium calculations of the composition distribution of sodium. The conclusions and implications are described in the last chapter of this thesis.

Thesis Declaration

This work contains no material which has been accepted for the award of any other degree or diploma in any university or other tertiary institution to myself, Woei Lean Saw, and, to the best of my knowledge and belief, contains no material previously published or written by another person, except where due reference has been made in the text.

I give consent to this copy of my thesis when deposited in the University Library, being made available for loan and photocopying, subject to the provisions of the Copyright Act 1968.

I acknowledge that copyright of published works contained within this thesis (as listed in List of Publications, page xi) resides with the copyright holder(s) of those works.

I also give permission for the digital version of my thesis to be made available on the web, via the University's digital research repository, the Library catalogue, the Australasian Digital Theses Program (ADTP) and also through web search engines, unless permission has been granted by the University to restrict access for a period of time.

Woei Lean Saw, 5th June 2009

List of Publications

Paper I W.L. Saw, G.J. Nathan, P.J. Ashman, Z.T. Alwahabi, Assessment of the release of atomic Na from a burning black liquor droplet using quantitative PLIF, Combustion Flame 156 (2009) 1471–1479.

Paper II W.L. Saw, G.J. Nathan, P.J. Ashman, Z.T. Alwahabi, M. Hupa, Simultaneous measurement of the surface temperature and the release of atomic sodium from a burning black liquor droplet, revised version submitted to Combustion and Flame on 10th November 2009.

Paper III W.L. Saw, G.J. Nathan, P.J. Ashman, M. Hupa, Influence of droplet size on the release of atomic sodium from a burning black liquor droplet in a flat flame, submitted to Fuel on 5th June 2009.

Paper IV W.L. Saw, M. Forssén, M. Hupa, G.J. Nathan, P.J. Ashman, The influence of boron on the emission of sodium during burning black liquor combustion under oxidative conditions, Appita J. 62 (3) (2009) 219–225.

Paper V W.L. Saw, G.J. Nathan, P.J. Ashman, M. Hupa, Influence of stoichiometry on the release of atomic sodium from a burning black liquor droplet in a flat flame with and without boron, Fuel, 10.1016/j.fuel.2009.11.023.

Acknowledgements

"Gratitude is when memory is stored in the heart and not in the mind.

Lionel Hampton

The completion of this thesis could not have been achieved without the contributions and support from those people listed below.

I would like express my gratitude to my principal supervisor, Professor Graham (Gus) Nathan, for providing me the opportunity to do research in such interesting areas of black liquor combustion incorporated with a laser diagnostic technique. I really appreciate his unwavering guidance, confidence and support throughout my PhD candidature. Thank you Gus. Dedicated support from my first co-supervisor, Dr. Peter Ashman, in constantly providing me with the insight into kinetics, and also his supervision is gratefully acknowledged. Dr. Zeyad Alwahabi, my second co-supervisor, has always provided valuable support in the area of laser diagnostic, and his supervision is also gratefully acknowledged.

All the financial support is gratefully acknowledged. Support for this work was provided by several sources: the Divisional Scholarship from the Faculty of Engineering, Computer and Mathematical Sciences (ECMS) at The University of Adelaide, School of Mechanical Engineering, Australian Research Council, Adelaide Graduate Centre and Åbo Akademi Process Chemistry Centre (ÅA-PCC).

Special thanks to Philip van Eyk who assisted with the experimental setup and data processing. Also thanks to Paul Medwell who assisted with the data processing. The technical support from Silvio De Ieso and Billy Constantine from the School of Mechanical Engineering are greatly appreciated. I would also like to thank the officemates of room S216 and the rest of the postgraduate students and staff of Schools of Mechanical and Chemical Engineering for making my PhD candidature so pleasant.

This work has been undertaken as part of a broader collaboration with Professor Mikko Hupa of ÅA-PCC. I would like to acknowledge him for giving me such valuable opportunities to visit PCC, as well as his supervision and support during the stay. Also, his valuable comments on joint publications are gratefully acknowledged. I want to thank Mr. Mikael Forssén, a previous member of ÅA-PCC, for his supervision, and also the friendly staff of ÅA-PCC for making my stay in Finland so enjoyable.

The editors and the anonymous journal reviewers are gratefully acknowledged for their insight comments on each of the papers listed in this thesis.

My Aussie family, the Yongs, especially Elizabeth, have always been available to give advice on English language and to share my ups and downs. This is greatly appreciated and unforgettable. Thank you.

Last but not least, I want to express my gratitude to my wife, Kai Lin and my family for their endless love and encouragement throughout the journey of completing this thesis. Thank you.

Woei Lean SAW

Summary of Each Paper

Paper I

This paper reports the development of the simultaneous measurements of planar laser-induced fluorescence (PLIF) and absorption technique to measure release of atomic sodium at high concentration during the combustion of black liquor. This technique was incorporated with an iterative correction to correct for fluorescence trapping and collisional quenching. The concentration of atomic sodium measured by the PLIF was compared with an independent first-order kinetic model. The values of the models were found to be higher than the values obtained from the PLIF, giving confidence that the correction, while high, is not excessive. The incorporation of the correction allows reliable measurement of the distribution of atomic sodium by PLIF at concentrations of 1 ppm, as can occur during black liquor combustion The concentration of atomic sodium during the stages of drying, devolatilisation and char combustion is an order of magnitude less than that in the smelt phase, of the order of 0.1 ppm in the present experiments.

Paper II

This paper reports the simultaneous measurements of the release of atomic sodium during the burning of a black liquor droplet, and its surface temperature, using PLIF and two-dimensional two-colour optical pyrometry techniques. A series of 10 mg black liquor droplets were burned in the flame provided by the flat flame burner at two flame conditions, fuel lean (Ø = 0.8), and fuel rich (Ø = 1.25). This study found that the surface temperature distribution is significantly non-isothermal. The study also found that the release of atomic sodium during the drying and devolatilisation stages was

correlated with the external surface area (or swelling). The paper also presents the first statistical analysis of surface temperature on a burning black liquor droplet.

Paper III

This paper reports the influence of initial droplet size on the temporal release and the release rate of atomic sodium during the burning of a black liquor droplet in a flat flame environment. Three different initial diameters of black liquor droplets, 1.3 mm (~2 mg), 1.7 mm (~5 mg) and 2.2 mm (~10 mg) were burned in a flat flame at equivalence ratios ($Ø_{bg}$) of 0.8, 0.9 and 1.25. A key finding of this study is that the relationship between the period of each of the combustion stages and the initial diameter is approximately parabolic. This demonstrates that the periods are dependent on the external surface area of the droplet. The total release of atomic sodium is greatest during the smelt coalescence stage and was found to be independent from initial droplet size compared with the stages of drying, devolatilisation and char combustion. In addition, the release rate of atomic sodium was found to be dependent upon initial diameter for all the black liquor combustion stages.

Paper IV

This paper reports the influence of boron on the emission of sodium during black liquor combustion under oxidative conditions within a single droplet furnace (SDF). A series 10 mg black liquor droplets were burned within the SDF at 900, 1000 or 1050ºC. The gaseous environment within the SDF was N_2 with oxygen added at a concentration of 2, 5 or 10 vol %. The loss of sodium was deduced by the difference between the initial sodium concentration and the sodium concentration left in the residue at specific exposure times. One of the key findings is that the difference between the sodium loss from the black liquor with and without boron increases at 900ºC, especially for higher oxygen concentrations. However, the difference between the sodium loss from the black liquor with and without boron decreases above 1000ºC. The addition of boron in black liquor also alters the characteristic combustion times.

Paper V

This paper reports the influence of boron on the temporal release of sodium during the burning of a black liquor droplet using the simultaneous measurements of PLIF and absorption techniques. A series of 10 mg black liquor droplets with or without boron were burned in the flame provided by the flat flame burner at three flame conditions, fuel lean ($Ø_{bg}$ = 0.8 and 0.9), and fuel rich ($Ø_{bg}$ = 1.25). One of the key findings was that the addition of boron to black liquor does not alter the trend of the release of atomic sodium. However, the trends are influenced by $Ø_{bg}$ (i.e. the excess oxygen) in the flame. The addition of boron to the liquor clearly reduced the total atomic sodium released, especially during the char consumption stage under oxidising conditions.

Chapter 1

Introduction

"Research is to see what everybody else sees, and to think what nobody else has thought."

Albert Szent-Gyorgyi

Biomass is a feasible alternative to fossil fuel for energy generation although it cannot displace all fossil fuel usage. In 2006, the world's total energy consumption had increased by almost 25% over the previous two decades [1]. Approximately 87% of that energy was supplied by the use of fossil fuels such as petroleum, natural gas and coal, while less than 1% of that energy was supplied by renewable sources [1], as shown in Figure 1.1, where the renewable energy is predominantly geothermal, solar, wind and wood and waste. The increase in global consumption of energy from fossil fuels is matched by a proportional increase in carbon dioxide (CO_2) emissions, considered to be a major contributor to global warming [2]. Since the forecast world energy demand has increased annually by 2% [3] the use of biomass is expected to be a significant alternative source of energy to meet the demand without increasing the present level of CO_2. Biomass is a sustainable and renewable source of energy with close to no net releases of CO_2 (or CO_2 neutral) [4], and with the flexibility and cost effectiveness to convert to transportation fuel [4–5], or electricity [6]. Other sources of renewable energy are unlikely to offer the same advantages. Biomass refers to all organic material

that stems from plant material (including algae, trees and crops) [6], with wood as the main representative [7]. Biomass consists of a mixture of hemicellulose, cellulose, lignin and extractives [6].

NOTE:
This figure is included on page 2 of the print copy of the thesis held in the University of Adelaide Library.

Figure 1.1 The average distribution of world's total energy consumption from 1986 to 2006 [1].

The by-product of the pulp and paper industry is a source of energy. The pulp and paper industry is one of the manufacturing sector's largest consumers of fossil fuel and one of the largest self-generator of energy. The pulp and paper industry generates 50% of its energy needs from wood residue and the by-product, black liquor [8], which consists of water and both organic components of wood (mainly lignin), and inorganic components, derived from sodium-based pulping chemical [9], as shown in Table 1.1 [10]. Black liquor is conventionally burned in a kraft recovery boiler both to recover the pulping chemicals for the pulping process and heat. Conversion of the black liquor into high pressure steam drives the turbines, which generate electricity to meet the paper mill's energy requirements. Recently, black liquor gasification technology has been developed to improve the recovery efficiency of the heat generated from the black liquor organic components [11–12]. Black liquor is also being considered as a potential feedstock for an alternative transport fuel. The black liquor gasification for motor fuels production (BLGMF) is presently under development with a view to replacing conventional

recovery boilers. This process converts black liquor to biomass-based methanol and dimethyl-ether (DME) [13].

Table 1.1 Typical propositions of the organic and inorganic compounds in black liquor [10].

NOTE:
This table is included on page 3 of the print copy of the thesis held in the University of Adelaide Library.

Kraft pulping, a type of chemical pulping process, is the most common method used in the industry to produce wood pulp. A schematic diagram of the kraft pulping process is as shown in Figure 1.2. In the kraft pulping process, a chemical solution, known as white liquor (pulping chemicals), consisting of sodium hydroxide (NaOH) and sodium sulfide (Na_2S), is used to dissolve the lignin that holds the cellulose fibres together in a heated digester [14]. The mixture of pulp and chemical waste is removed from the digester and the pulp is cleaned in a brownstock washer. The waste is converted into black liquor in an evaporator, whereas the pulp is then converted into paper. Typically at least 70% of the water content is evaporated, depending on the requirement of the recovery boiler, in order to achieve high thermal efficiency [15]. The black liquor is sprayed into a kraft recovery boiler, typically as droplets from 0.5–5 mm in diameter [9, 16].

In a recovery boiler, the organic components are converted to heat through a pyrolysis process during the in-flight burning of the black liquor droplets. The residue, mainly char (carbon) and inorganic components, then falls to the char bed at the bottom of the boiler, where the char is consumed and the inorganic compounds formed into a smelt. Some of the char is consumed during the reducing process of the oxidised inorganic components, notably sodium sulphate (Na_2SO_4), and converted to Na_2S. The smelt is

transferred and dissolved in water to form green liquor, which consists of sodium carbonate (Na_2CO_3) and Na_2S. The Na_2CO_3 in the green liquor is then converted into white liquor in a causticizing process, in which calcium oxide, CaO (i.e. lime) is added to convert sodium carbonate into NaOH [14]. The energy intensive causticizing process can be reduced by the autocausticizing proposed by Janson [17]. The concept of autocausticizing is to add boron into the kraft pulping cycle, where it reacts with molten Na_2CO_3 and then dissolved in water to form white liquor without going through the conventional causticizing process.

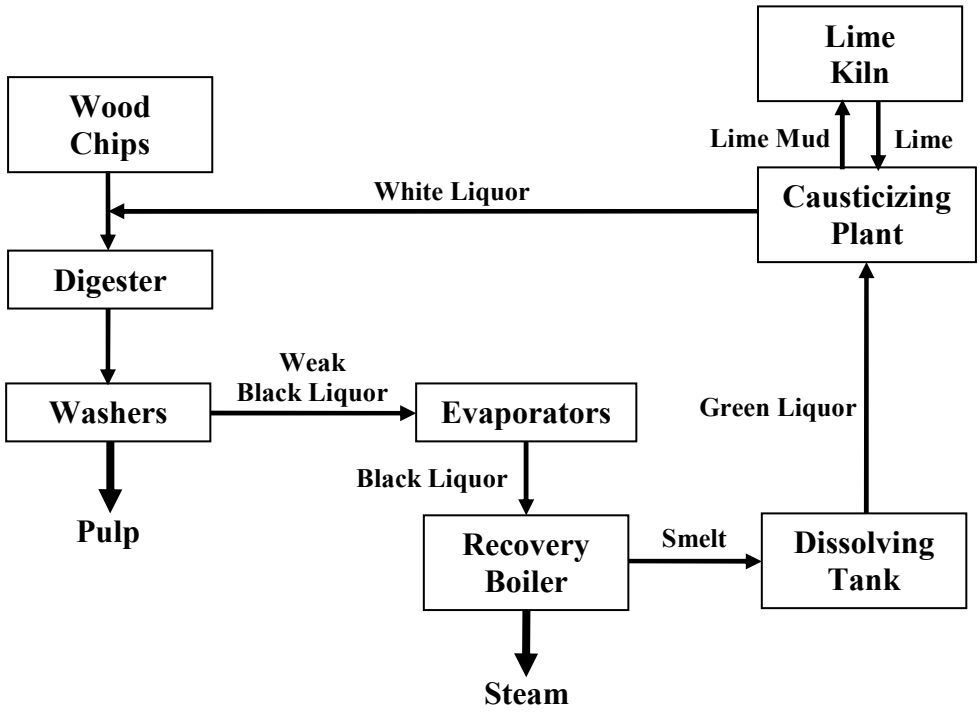

Figure 1.2 Schematic diagram of the kraft pulping process.

One of the major unresolved issues in a recovery boiler is the deposition of alkali salts, mainly sodium compounds released during the combustion of black liquor. These deposits form on the surface of heat exchanger tubes in the upper furnace, causing fouling and corrosion, especially to the superheaters. They reduce the effectiveness of heat transfer, cause material failure, and also lower overall black liquor throughput rates [18–20]. To understand and improve the design and operation of recovery boilers, computational fluid dynamics (CFD) can potentially be applied as a tool. These CFD tools can be used to investigate the flow patterns, locations where combustion of the

reaction occurs, pollutant formation processes, and heat release of gas and droplets of black liquor in a recovery boiler [18, 21–25]. Once validated, the CFD predictions can be used to develop improved design and/or operation at various conditions, at a relatively low cost. Sufficiently accurate, numerical efficient sub-models required for each relevant process to be assessed [25] are not presently available. The findings present here of the temporal release and the release rate of sodium during each stage of black liquor combustion can therefore provide new information for the development of key parameters for the CFD model to optimise the sodium chemistry in a kraft recovery boiler, owing to the unique the combustion of each particle.

Many studies on the release of sodium from black liquor combustion have been conducted. However, these are all indirect being based on the analysis of the sodium left in the residue. Other researchers have used the chemical equilibrium approach to predict fume formation in the lower furnace. Importantly, no direct measurement of the release rate or temporal release of atomic sodium from black liquor is available because it cannot be measured directly in the reactors or obtained from chemical equilibrium calculations.

The objective of this study is to provide new information on the release rate and the temporal release of atomic sodium, which can be used to support the development of reliable sub-models. To measure the release rate of atomic sodium it is necessary to investigate sodium in its atomic form. Detailed aims are presented in turn within each paper.

Chapter 2

Background

"I can't change the direction of the wind, but I can adjust my sails to always reach my destination."

Jimmy Dean

2.1. Black liquor

As described in the introduction, black liquor is the by-product of the kraft pulping process, and a complex, important source of renewable fuel in the pulp and paper industry. Black liquor has a very high sodium concentration at approximately 20 wt% (dry), much higher than other solid fuels such as coal, biomass and wood, in which it typically spans 0.001–5 wt% (dry) [26–28]. The sodium can be bound to both organic and inorganic compounds [29]. During black liquor combustion the organically bound sodium, which is associated with the phenolic hydroxyl and carboxyl compounds, decomposes and converts to Na_2CO_3 [29].

Combustion of a single droplet of black liquor combustion can be divided into the four stages of drying, devolatilisation, char combustion and smelt oxidation [30], as shown in Figure 2.1. The initial three stages of black liquor combustion are similar to those of other solid fuels, such as coal and wood [31–32]. Droplet burning in a recovery furnace takes place in both oxidising and reducing environments. During the drying stage, the

water content in the droplet is vaporized due to heat transferred to the droplet from the surroundings [31]. In addition, the diameter of the black liquor droplet increases by 50% from its original diameter [16, 30] due to expansion of the gases within the droplet [16].

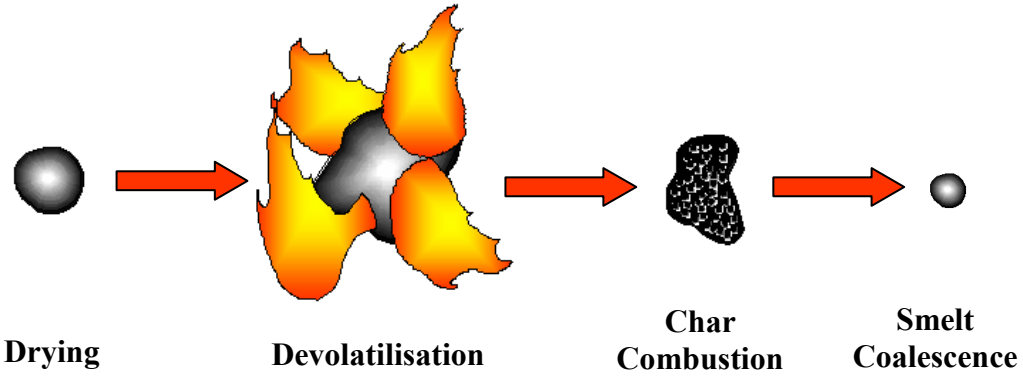

Figure 2.1 A schematic diagram of the four stages of black liquor combustion.

During the devolatilisation stage, the droplet undergoes thermal degradation and releases volatile gases [33]. The volatile gases are subsequently burned, which causes the characteristic bright yellow flame around the droplet, indicating the beginning of the devolatilisation stage. The disappearance of the flame indicates the end of this stage [30]. Hence, the surrounding gaseous furnace environment does not significantly influence the behaviour of the droplet during this stage as the droplet creates a gas environment of its own [30]. The droplet swells to its maximum size at the end this stage by 10-60 times in volume [34] due to gas evolution within the highly viscous droplet [31]. The swelling ratio of black liquor is liquor-dependent and it is independent of droplet size or the initial dry solids content [34]. The swelling effect increases the external surface area and has a significant impact on the burning times [34–35]. Overlapping combustion in the drying and devolatilisation stages can occur due to large temperature gradients within the swollen droplet (Biot number, Bi > 1) [31, 36]. Here, the Bi >1 refers to the large thermal response of internal temperature of the droplet to its surface temperature [37]. After all the volatiles in the droplet have been released the large swollen and porous char undergoes heterogeneous reactions, which are subsequently influenced by the gaseous environment [30].

During the char combustion stage, char is oxidised by reaction with H_2O, CO_2 [38–39], O_2 [31, 40], and by the reduction of Na_2CO_3 and Na_2SO_4 [31, 40], as shown in Equations 2.1 to 2.5. The rates of char oxidation and gasification increase at above 1000ºC due to the catalytic effect of sodium in the droplet on the char [40].

$$C\ (s) + H_2O\ (g) \rightarrow CO\ (g) + H_2\ (g) \quad (2.1)$$

$$C\ (s) + CO_2\ (g) \rightarrow 2CO\ (g) \quad (2.2)$$

$$C\ (s) + O_2\ (g) \rightarrow 2CO\ (g) \quad (2.3)$$

$$2C\ (s) + Na_2CO_3\ (s, l) \rightarrow 2Na\ (g) + 3CO\ (g) \quad (2.4)$$

$$4C\ (s) + Na_2SO_4\ (s, l) \rightarrow Na_2S\ (s, l) + 4CO\ (g) \quad (2.5)$$

A molten bead of smelt, consisting of inorganic components (mainly Na_2CO_3 and Na_2S), is formed at the end of the char combustion stage and the oxidation of Na_2S can occur if O_2 is available [30] (Equation 2.6). The reaction of Na_2S to Na_2SO_4 can be determined by measuring the weight of the residue before and after the smelt oxidation. The weight of the residue is increased slightly by the smelt oxidation [40] because the molar weight of Na_2S is increased from 78 g/mol to 142 g/mol (Na_2SO_4).

$$Na_2S\ (s, l) + O_2\ (g) \rightarrow Na_2SO_4\ (s, l) \quad (2.6)$$

The above information was employed to identify the stages of black liquor combustion and its characteristics both in a flat flame as reported in **Papers I, II, III and V,** and within a closed furnace as reported in **Paper IV**.

2.2. Release of sodium during black liquor combustion

Ideally, all sodium in the black liquor droplet is recovered at the bottom of a kraft recovery boiler. However, some of the sodium is released from the droplets during the in-flight burning and from the char-bed reactions. The negative aspect of the release of the sodium vapour is that it can react with combustion products, such as CO_2 and SO_2 to form fume (<1 μm), consisting of Na_2CO_3 and Na_2SO_4 [41–45]. This fume can be

deposited on the upper furnace, causing fouling and corrosion that reduce the capacity of a recovery boiler [18–20]. Fume is difficult to capture and contributes to air pollution. Conversely, a beneficial aspect of the release of sodium vapour is that it can provide an important trap to capture sulphur in flue gases to form Na_2SO_4. That proportion which is collected in the particle filter, typically an electrostatic precipitator (ESP), can then be recycled to the process.

2.2.1. Measurement of the release of sodium

The study of sodium release is most relevant if assessed within the range of the droplet size sprayed into kraft recovery boilers i.e. from 0.5–5 mm in diameter. Most laboratory-scale studies of the release of sodium during the combustion of black liquor have been conducted in closed furnaces, which have the advantage of providing a well-defined gaseous environment and temperature field [41, 43–51]. Examples of the closed furnace systems commonly used are single droplet furnaces (SDF), laminar entrained flow reactors (LEFR) and heated grid reactors (HGR). The concentration of sodium emission during the combustion within a furnace is determined by the difference between the initial sodium concentration in the droplet and the sodium concentration left in the residue at a given exposure time. For example, the study by Volkov et al. [47] estimated the loss of sodium occurring during each stage of black liquor combustion based on 2 to 5 mm black liquor droplets. The mechanism of the release of sodium during each stage of black liquor combustion was later determined by several researchers [41, 43 and 45].

Frederick and Hupa [48] suggested that the sodium loss during devolatilisation is the most significant source of the fume formation, based on 8 to 20 mg of black liquor droplet. Later, the study by Verrill et al. [41] based on 2 mm average diameter droplet identified that the significant loss of sodium during the devolatilisation stage is caused by the physical ejection of droplet fragments. This proposition has been supported by the study of Kauppinnen et al. [46] who used several different reactors of SDF, LEFR and HGR, and measuring devices such as a tapered element oscillating microbalance (TEOM), an electrical low pressure impactor (ELPI) and a Berner-type low pressure impactor (BLPI), to conclude that approximately 10% of the sodium mass loss from

those large black liquor droplets occurs by the physical ejection during the devolatilisation stage. Note that the measuring devices are used to estimate both the distribution of micron-sized particles and mass concentration of particles in the product gas. The sodium concentration is then determined by analysing those samples with ion chromatography (IC). The droplet sizes were 95 to 125 micron for LEFR and HGR devices and 20 mg for SDF systems. These 'ejecta' or intermediate-size particles, ISP, (1–100 μm) are much more likely to undergo char combustion and smelt oxidation in the free board above the bed to release sodium into the upper furnace. This physical ejection mechanism may potentially be avoided in a kraft recovery boiler by introducing the black liquor at droplet sizes in the range of 100 micron. However, this approach is not possible for the present configuration of a kraft recovery boiler.

Li and van Heiningen [45] have proposed that the most significant release of sodium vapour occurs during the char combustion stage based on 10 mg of 37 micron powdered black liquor solids, and is due to the decomposition of Na_2CO_3 by carbon, as shown in Equation 2.7. The study by Cameron [43] concluded that significant sodium vapour is released during the smelt reaction between Na_2S and Na_2CO_3 under oxidising conditions, as shown in Equation 2.8. Interestingly, physical ejection can also occur during the char combustion stage under oxidising environments [47, 49 and **Paper IV**] and the smelt oxidation stage [30]. The initial droplet diameters used in those studies were above 1 mm.

$$Na_2CO_3\ (s, l) + C\ (s) \leftrightarrow 2Na\ (g) + CO_2\ (g) + CO\ (g) \qquad (2.7)$$

$$Na_2S\ (l) + 4Na_2CO_3\ (l) \leftrightarrow Na_2SO_4\ (l) + 4CO_2\ (g) + 8Na\ (g) \qquad (2.8)$$

The previous measurements employed for the analysis of sodium concentration for the residue do not provide the temporal history of the release of sodium during the black liquor combustion because sodium vapour is unstable and cannot be measured directly in the outlet gases from the reactors. However, these sodium release mechanisms were adopted in **Papers I to V** to identify the release of sodium at different stages. The concept of the smelt analysis was also adopted in **Papers I, III and V** to measure the total sodium emission and to compare that with the release of atomic sodium.

Another method has been previously employed to measure the concentration of sodium in the flue gas with a Recovery Boiler Dust Analyzer (RBDA) [52]. The RBDA dissolves a flue gas sample in ion-exchanged water and the sodium concentration is determined by the Ion-Selective Electrode in the device. The recent mill study by Tamminen et al. [53] shows that 90-95% of the fuming occurs during the in-flight burning of black liquor droplets and only 5-10% of the fume originating from the char bed was deduced. The fume formation could result from the physical ejection from the in-flight burning droplets. However, the temporal release or the release rate of atomic sodium from black liquor cannot be measured directly from the flue gases. Hence, the investigation of both the temporal release and the release rate of atomic sodium are reported in **Paper II and III**.

Previously, Verrill and Wessel [21] have modelled the influence of droplet size and furnace temperature on the sodium loss from physical ejection. However, this model needs to be validated with experimental results. Hence, the influence of droplet size on the concentration release of atomic sodium during each stage of black liquor combustion is conducted and reported in **Paper III**.

2.2.2. Equilibrium and kinetic calculations on the release of sodium

A chemical equilibrium approach was implemented by Pejryd and Hupa [54] to predict the fume formation in the lower furnace. They suggested that the major gas-phase sodium species within this region are atomic sodium (Na) and sodium hydroxide (NaOH), as shown in Figure 2.2, which is consistent with findings of Borg et al. [42]. These studies suggest that atomic sodium could be a major contributor to fume formation. This equilibrium calculation approach has also been adopted in the study by Saw et al. [55] to calculate the composition of the sodium species from the combustion of a black liquor droplet in a flat flame. The resulting calculation that Na (g) and NaOH (g) are the two major sodium species agrees with the previous studies. These calculations, however, only provide the composition of species and concentration under specified conditions at equilibrium. Hence, information on the release rate of atomic sodium from black liquor cannot be obtained from chemical equilibrium approaches.

The present investigation also employs a kinetic model of sodium concentration, developed using the Plug Flow Reactor (PFR) model in CHEMKIN 4.1 with GRI-Mech v3.0 [56] in conjunction with the kinetic data for reactions of Na, hydrogen (H), oxygen (O) and sulphur (S) obtained from References [57–59], as reported in **Paper I**. This model was used to estimate the composition of combustion gases (from the combustion of the natural gas and air) entrained into the sodium plume that is released from the black liquor particle. The input sodium concentration of the kinetic model was obtained independently from the smelt analysis, and the entrainment of the combustion gases into the sodium plume was determined by the method of the similarity solutions for a fully developed jet flow conducted by Becker et al. [60]. This model is then compared with the atomic sodium measured by the PLIF technique. Details of the comparison are discussed in **Paper I.**

Figure 2.2 Lower furnace equilibrium compositions for normal, “open cycle” liquor as function of temperature. Air-to-fuel ratio = 70% (the fuel corresponds to the black liquor) [54].

2.3. Autocausticizing

In the kraft pulping process, the white liquor (cooking chemical) is conventionally produced by a causticizing process, in which Na_2CO_3 in the green liquor reacts with slaked lime, $Ca(OH)_2$ to form NaOH (aq) and lime mud, calcium carbonate ($CaCO_3$), as

shown in Equations 2.9 and 2.10. The NaOH is then separated from the $CaCO_3$ and is transferred to the digester and used as the cooking chemical. The $CaCO_3$ is converted back to CaO (Equation 2.11) in an energy intensive lime kiln.

Causticizing process:

$$CaO\ (s) + H_2O\ (l) \leftrightarrow Ca(OH)_2\ (s) \quad (2.9)$$

$$Ca(OH)_2\ (s) + Na_2CO_3\ (aq) \leftrightarrow 2NaOH\ (aq) + CaCO_3\ (s) \quad (2.10)$$

$$CaCO_3\ (s) \xleftrightarrow{Heat} CaO\ (s) + CO_2\ (g) \quad (2.11)$$

The concept of autocausticizing is to add a chemical compound into the kraft pulping cycle, where it reacts with molten Na_2CO_3 and is then dissolved in water to form white liquor without going through the causticizing process. The autocausticizing agents include various metal oxides, silicates, phosphates and borates [17, 61–62].

2.3.1. Autocausticizing using sodium borates

The study by Janson [17, 61–62] has proposed that the use of sodium borates is the most suitable autocausticizing agent due to its acceptable production of quality pulping liquor. The process and the schematic diagram of borates autocausticizing by Janson [17, 61–62] is as shown in Equations 2.12 and 2.13 and Figure 2.3, respectively. Later, this particular process was found to be not technically feasible to apply in a full scale autocausticizing due to large amount of borate in the kraft pulping cycle, which lowers the heating value of black liquor and increases the liquor viscosity [63]. Also, the high cost of the make-up chemical of boron further limits the full application [63].

Autocausticizing process:

$$2NaBO_2\ (s, l) + Na_2CO_3\ (s, l) \leftrightarrow Na_4B_2O_5\ (s, l) + CO_2\ (g) \quad (12)$$

$$Na_4B_2O_5\ (s, l) + H_2O\ (l) \leftrightarrow 2NaOH\ (aq) + NaBO_2\ (aq) \quad (13)$$

NOTE:
This figure is included on page 15 of the print copy of the thesis held in the University of Adelaide Library.

Figure 2.3 Schematic diagram of the kraft pulping process with borate autocausticizing proposed by Janson [17, 61–62].

2.3.2. Partial autocausticizing using sodium borates

The original autocausticizing approach was later refined by Tran et al. [64] to increase the effectiveness of boron on the causticizing process by partial autocausticizing. In the partial autocausticizing process, less boron is added to the pulping cycle than for the autocausticizing approach of Janson [17, 61–62]. The reactions of boron take place in the recovery boiler, primarily in the smelt phase when sodium metaborate ($NaBO_2$) reacts with a part of the molten Na_2CO_3 to form trisodium borate (Na_3BO_3) and CO_2, as shown in Equation 2.14 [64]. The percentage of metaborate conversion through the decarbonisation reactions between $NaBO_2$ and Na_2CO_3 increases as the temperature is increased [65]. The Na_3BO_3 then forms NaOH, thereby regenerating the $NaBO_2$ as shown in Equation 2.15, when the smelt is dissolved into the green liquor [64]. The residual Na_2CO_3 reacts with lime in the causticizing process to form NaOH. Recently, two mills trials have demonstrated that addition of boron can debottleneck the causticizing plant by a reduction in lime usage [66–67]. This result promises to be a cheaper alternative than upgrading the existing plant.

$$NaBO_2\,(s, l) + Na_2CO_3\,(s, l) \leftrightarrows Na_3BO_3\,(s, l) + CO_2\,(g) \qquad (2.14)$$

$$Na_3BO_3\,(s, l) + H_2O\,(l) \leftrightarrows NaBO_2\,(aq) + 2NaOH\,(aq) \qquad (2.15)$$

Many studies have been conducted on the effects of the addition of boron into the kraft recovery cycle. The addition of boron influences the swelling characteristics of the black liquor and the melting temperature of the smelt. In one recent study [68], the characteristic swelling during the combustion of black liquor was shown to increase slightly at low boron additions (~10% autocausticizing), and to reduce at higher additions. The swelling influences the burning time, being slightly shorter at low additions and longer at high additions of boron than for black liquors without boron [68]. The Na_3BO_3 is readily soluble in the smelt, consisting of Na_2CO_3, Na_2S and sodium chloride (NaCl), and changes the overall melting properties of the salt mixtures as has been calculated using a thermodynamic approach [68]. The presence of boron reduces the melting temperature of the smelt. This effect could increase the rate of fouling and corrosion in the upper furnace if significant quantities of boron were to be added into the cycle [68]. Tran et al. [65] have suggested that the decarbonation of Na_2CO_3 can be enhanced by the presence of char carbon as shown in their complicated combined reaction Equation 2.16. However, the addition of boron to black liquor reduces the char bed temperature due to the endothermic nature of the autocausticizing reaction [65]. This information is utilised in **Papers IV and V**.

$$Na_2CO_3\ (s, l) + NaBO_2\ (s, l) + C\ (s) \rightarrow Na_3BO_3\ (s, l) + 2CO\ (g) \qquad (2.16)$$

2.3.3. Influence of boron on the release of sodium

The influence of boron on the characteristics of black liquor combustion and melting temperature may directly or indirectly influence the fume formation due to the alteration of the release of sodium from the black liquor combustion with boron. Two mill trials have demonstrated that addition of boron to the black liquor reduced fume formation [66–67]. As a consequence, the concentration of SO_2 in a boiler from the combustion of black liquor with boron was reported to be higher than that without boron [66, 69]. While this suggests that the addition of boron may influence the release of sodium during black liquor combustion, no systematic study has been conducted on the influence of boron on sodium emission. Hence, an investigation of the influence of boron on total sodium emissions during the combustion of a black liquor droplet under oxidative conditions is reported in **Paper IV**.

Previously, a study based on thermogravimetric measurements conducted by Janson [62] has suggested that sodium vapour can be released from the decomposition of the smelt containing boron at the temperature of 1000–1100ºC. Neither the dependence of the sodium release on the amount boron in the liquor nor the decomposition of a smelt containing boron is well understood. Hence, **Paper V** reports on the release of atomic sodium from during each stage of black liquor combustion with boron and compares it with that without boron.

2.4. Implementation of laser diagnostics technique on the release of alkali metal from solid fuel

Laser diagnostic techniques have distinct advantages over the conventional sampling techniques to quantify the release of alkali metal from a burning solid fuel(s). This is because laser diagnostic techniques can be used to provide instantaneous quantitative measurement of a specific species concentration without influencing the combustion process. Examples of laser diagnostic techniques that have been successfully used in the study of alkali release from burning solid fuels (coal and biomass) are excimer laser-induced fragmentation fluorescence (ELIF) [70–76], plasma excited atomic resonance line spectroscopy (PEARLS) [77–78], laser-induced fluorescence (LIF) [79–80], and laser-induced breakdown spectroscopy (LIBS) [81–82]. The LIF technique was selected for the present study because it is able to provide the two-dimensional quantitative release of atomic sodium and the release rate of atomic sodium throughout the combustion of a solid fuel, as is demonstrated in Ref. 80. This distinguishes it from other techniques, which provide the final forms of sodium released.

2.4.1 Laser-induced fluorescence (LIF)

Laser-induced fluorescence (LIF) is well established for atomic and molecular species detection. This is because each species (atomic or molecular) has one or more unique absorption lines that are not shared by other species (depending on the system). The laser wavelength is tuned to match the chosen absorption line of target species. A

photon of energy is then absorbed, bringing that species to the excited state. In this state, the excited atom or molecules then decay spontaneously, emitting another photon of energy or fluorescence at the same or different wavelength from that of the laser wavelength [83–84], as shown in Figure 2.4. The fluorescence signal can then be recorded using a monochromator or an intensified charged-couple device (ICCD) camera. This LIF technique may also applied to measure temperature, velocity and pressure for studying complex combustion processes [85]. The LIF technique has been applied in various fields, such as the measurement of the concentration of NO, an important combustion-generated pollutant during the combustion process [86], and to measure the two-dimensional temperature distribution in the compression stroke of a spark-ignition engine [87].

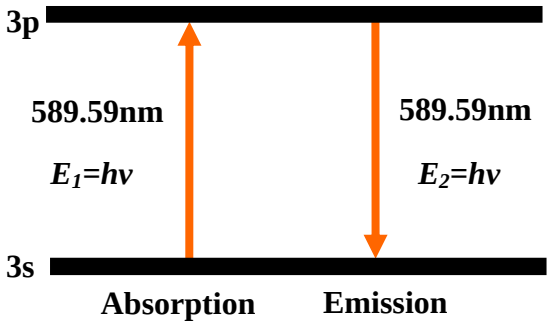

Figure 2.4 Example of sodium (D_1) atom energy level diagram.

2.4.1.1. The implementation of LIF on the release of atomic sodium

Previous studies of atomic sodium in flames have been conducted using point measurements of LIF to determine the concentration [59, 88–89] and to assess the complex chemistry of sodium in a flame at various gas conditions [59, 89]. This measurement technique has a disadvantage in assessing the sodium plume of a burning black liquor droplet, since the process is unsteady and the combustion of each swelling particle is unique. The one-dimensional nature of this method limits the capacity to resolve spatial and temporal distributions. Recently, a planar method was employed in our laboratory to allow the quantitative measurement of atomic sodium in the plume of a burning coal particle, by van Eyk et al. [80]. This work established a relationship

between the number density of atomic sodium and the measured fluorescence signal by calibration against a known concentration of sodium solution. The number density of atomic sodium was determined by the Beer-Lambert law and the fluorescence signal was measured directly from the sodium plume using an intensified charge-coupled device (ICCD) camera [80]. However, the concentration of sodium in coal is much less than in black liquor. The maximum concentration of atomic sodium for which quantitative data could be obtained by the method is 80 ppb [80], which was limited by the seeding approach and the large area of the flat flame burner. This calibration technique cannot be applied directly to black liquor. Hence, a new approach was needed to enable quantitative measurement of concentrations found in the plume of a black liquor droplet. The new method is reported in **Paper I**.

2.4.1.2. Limitation of LIF

The study by Daily and Chan [88] has demonstrated that the effect of trapping on the fluorescence signal will become significant if the concentration of atomic sodium in the flame (or the total absorptance) exceeds a threshold of 0.2 ppm (0.08 for the absorptance). The relationship between the fluorescence trapping and the absorption measured within the sodium plume was found to be non-linear, as shown in Figure 2.5. This is because when the fluorescence leaves the measurement volume, a proportion of it will be absorbed and attenuated by sodium atoms along the path to the collection optics [90]. Furthermore, collisional quenching of the laser exited atomic sodium by other major gas components present in a flame, such as N_2, CO_2 and O_2, influences the PLIF signal [91]. Hence, the development of an iterative method to correct for fluorescence trapping and collisional quenching was needed to enable quantitative measurement of atomic sodium. This correction was obtained by adapting the correction method developed by Choi and Jensen [92] to correct the measured laser induced incandescence (LII). Details of the development of the measurement of the high concentration of released atomic sodium during the combustion black liquor are reported in **Paper I**.

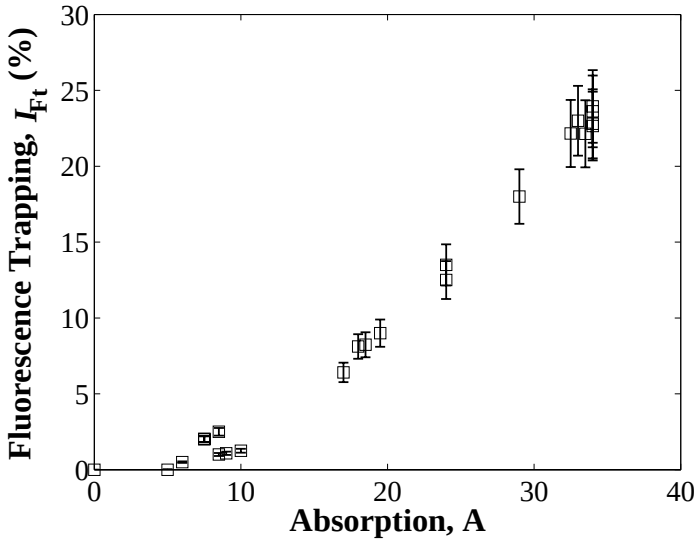

Figure 2.5 The variation of fluorescence trapping with absorption [**Paper I**].

2.5. Surface temperature

The release of the alkali metals, chlorines and sulphur compounds from black liquor is influenced by particle temperature [93]. The increase particle temperature is the result of combustion involving homogeneous and heterogeneous reactions, heat and mass transfer, and two-phase fluid flow [94–95]. Therefore, the temperature of a burning black liquor droplet is an important parameter for a better understanding of the phenomenon, and in the development of a recovery boiler model. Two-colour optical pyrometry has been well-established and widely used to measure the surface temperature at a single point on burning solid particle(s), mainly for coal [94–101], but also to measure soot temperature [102–105] and flame temperature [106–107]. The two-colour optical pyrometry adopted Planck's law and Wien law approximation (most commonly used), as shown below, to determine a particle temperature by measuring the relative emission intensity (emittance) at two wavelengths and relates the ratio to the temperature of the source [97]. To obtain the emittance, a narrow bandpass interference filter was placed in front of each of the two pyrometers. The technique was further improved by Stenberg et al. [93] to measure the surface temperature of a burning black liquor droplet in a hot, radiating environment. The technique was further adapted by Frederick et al. [108] to study the influence of oxygen on the surface temperatures of a burning black liquor particle, again at a single point. Later, a detailed simultaneous

study of the swelling, mass loss and the surface and internal temperatures of a burning black liquor droplet were measured by Ip et al. [109]. A digital video camera fitted with two infra-red filters was used to measure the surface temperature by detecting the radiation emitted from the burning black liquor droplet at two wavelengths [109]. This technique requires the grey emissivity (ε) of the droplet to be assumed. Nevertheless, it provided two-dimensional imaging of the surface temperature of a burning black liquor droplet.

The surface temperature of a burning black liquor droplet in the present study was determined by the two-colour pyrometry technique as describe above. Wien's law approximation, as shown in Equation (2.17), is selected as it relates to the emission intensity (E_λ) of a black body to the wavelength (λ) and absolute surface temperature (T_s).

$$E_{\lambda i} = -C_1 \lambda_i^{-5} \varepsilon_{\lambda i} \exp-\left(\frac{C_2}{\lambda_i T_s}\right) \qquad (2.17)$$

where ε_λ is emissivity of the solid surface at wavelength λ_i and C_1 and C_2 are first and second Planck's constants. The relationship between the ratio of two emission intensities, $E_{\lambda 1}$ and $E_{\lambda 2}$, at wavelengths, λ_1 and λ_2, respectively, are as shown in Equation (2.18). The T_s as shown in Equation (2.19) can be determined by rearranging Equation (2.18). The present difference of the wavelengths of 100 nm is within the range of 20 and 120 nm used in two-colour pyrometery in previous studies [94, 97, 101, 107]. These wavelengths are sufficiently close to each other for, the ratio of corresponding spectral emissivity of the black liquor droplet, $\varepsilon_{\lambda 1}/\varepsilon_{\lambda 2}$, to be reasonably assumed to be approximately unity. Under such conditions, the differences between the spectral emissivities of the droplet are negligible [107] and minimise the effects of any sudden variation in the absorption spectra of the gases [97].

$$\frac{E_{\lambda 1}}{E_{\lambda 2}} = \frac{\varepsilon_{\lambda 1}}{\varepsilon_{\lambda 2}} \left(\frac{\lambda_2}{\lambda_1}\right)^5 \exp\left[\frac{C_2}{T_s}\left(\frac{1}{\lambda_2} - \frac{1}{\lambda_1}\right)\right] \qquad (2.18)$$

$$T_s = \frac{-C_2\left(\frac{1}{\lambda_{`1}} - \frac{1}{\lambda_{`2}}\right)}{\ln\left(\frac{\varepsilon_{\lambda 1}}{\varepsilon_{\lambda 2}} \frac{\lambda_2^5}{\lambda_1^5} \Big/ \frac{E_{\lambda 1}}{E_{\lambda 2}}\right)} \qquad (2.19)$$

Details of the simultaneous measurements of the temporal release of atomic sodium, swelling and droplet surface temperature as a function of time under fuel-rich and fuel-lean conditions are reported in **Paper II.** The assessment of the influence of surface temperature on the release of atomic sodium is also reported in **Paper II**.

References

1. *World total energy of primary energy consumption*, 1980-2006, Energy Information Administration.
2. S. Soloman, G-K. Plattner, R. Knutti, and P. Friedlingstein, Irreversible climate change due to carbon dioxide emissions, PNAS 106 (2009) 1704–1709.
3. International Energy Outlook 2008, Energy Information Administration.
4. A. Demirbas, Progress and recent trends in biofuels, Prog. Energy Combust. Sci. 33 (2007) 1–18.
5. M. Balat, H. Balat and C. Oz, Progress in bioethanol processing, Prog. Energy Combust. Sci. 34 (2008) 551–573.
6. P. McKendry, Energy production from biomass (Part I): overview of biomass, Bioresource Technol. 83 (2002) 37–46.
7. C.D. Blasi, Modeling chemical and physical processes of wood and biomass pyrolysis, Prog. Energy Combust. Sci. 34 (2008) 47–90.
8. Manufacturing energy consumption survey, Energy Information Administration.
9. T.N. Adams, General characteristics of kraft black liquor recovery boilers, Kraft Recovery Boilers, 1997, Tappi Press: Atlanta, Georgia, USA. pp. 3–38.
10. Black Liquor, *Material Safety Data Sheet*, Weyerhaeuser Company 2004.
11. E.G. Kelleher, Black liquor gasification and the use of the product gases in combined-cycle cogeneration – phase II, Tappi J. 65 (1985) 106–110.
12. P.J. McKeough, C.J. Fogelholm, Development of an integrated gasification-combustion-cycle process (IGCC) for black liquor, Proc. 1991 Int'l Symp. Energy and Environment, Espoo, Finland, 1991, pp 197–205.
13. T. Ekbom, M. Lindblom, N. Berglin and P. Ahlvik, Technical and commercial feasibility study of black liquor gasification with methanol/DME production as motor fuels for automotive uses, Altenar II Report, Contract No. XVII/4.1030/Z/01-087/2001, Dec 2003.
14. Babcock and Wilcox Ltd, Steam, 40th edition, London.

15. H. Muller-Steinhagen, and C.A. Branch, Heat transfer and heat transfer fouling kraft black liquor evaporators, Experimental Thermal and Fluid Science 14 (1997) 425–437.

16. A. Macek, Research on combustion of black-liquors drops, Prog. Energy Combust. Sci. 25 (1999) 275–304.

17. J. Janson, The use of unconventional alkali in cooking and bleaching. Part 1. A new approach to liquor generation and alkalinity, Paperi. Puu 59 (1977) 425–430.

18. R.A. Wessel and L.L. Baxter, Comprehensive model of alkali-salt deposition in recovery boilers, Tappi J. 2 (2) (2003) 19–24.

19. P. Mikkanen, E.I. Kauppinen, J. Pyykönen, J.K. Jokiniemie, M. Aurela, E.K. Vakkilainen, K. Janka, Alkali salt ash formation in four Finnish industrial recovery boilers, Energy Fuels 13 (1999) 778–795.

20. D.W. Reeve, H.N. Tran and D. Barham, Superheater fireside deposits and corrosion in kraft recovery boilers, Tappi J. 64 (5) (1981) 109–113.

21. C.L. Verril and R.A. Wessel, Detailed black liquor drop combustion model for predicting fume in kraft recovery boilers, Tappi J. 81 (9) (1998) 139–148.

22. J.K Jokiniemi, J. Pyykönen, P. Mikkanen and E.I. Kaupopinen, Modeling fume formation and deposition in kraft recovery boilers, Tappi J. 79 (7) (1996) 171–181.

23. R.A. Wessel, K.L. Parker, and C.L. Verrill, Three-dimensional kraft recovery furnace model: implementation and results of improved black-liquor combustion models, Tappi. J. 80 (10) (1997) 207–220.

24. B. Malmberg, L. Edwards, S. Lundborg, M. Ahlroth, and B. Warnqvist, Prediction of dust composition and amount in kraft recovery boilers, Tappi J. 4 (3) (2005) 28–32.

25. K.J. Wåg, V.V. Reis, W.J. Frederick, and T.M. Grace, Mathematical model for the release of inorganic emissions during black liquor char combustion, Tappi J. 80 (5) (1995) 135–145.

26. J. Hulston, G. Favas, A.L. Chaffe, Effect of temperature and pressure on the physico-chemical properties of MTE treated Loy Yang lignites, Fuel 84 (2005) 1940–1948.

27. J.N. Knudesen, P.A. Jensen, and K. Dam-Johansen, Transformation and release to the gas phase of Cl, K, and S during combustion of annual biomass, Energy Fuels 18 (2004) 1385–1399.

28. H.M. Westberg, M. Bystrom, and B. Leckner, Distribution of potassium, chlorine, and sulfur between solid and vapor phases during combustion of wood chips and coal, Energy Fuels 17 (2003) 18–28.

29. T.M. Grace, D.G. Sachs, and H.J. Grady, Determination of the inorganic composition of alkaline black liquors, Tappi J. 60 (4) (1977) 122–125.

30. M. Hupa, P. Solin and R. Hyöty, Combustion behaviour of black liquor droplets, J. Pulp Paper Sci. 13 (2) (1987) 67–72.

31. Wm.J. Frederick, and M. Hupa, Black liquor droplet burning processes, in: T.N. Adams, Kraft Recovery Boilers, Tappi Press: Atlanta, Georgia, USA, 1997 pp. 131–160.

32. C.J. Lawn, *Principles of combustion engineering for boilers*, Academic Press, London (1987).

33. R. Alén, Swelling behaviour of kraft black liquor and its organic constituents, Bioresource Technology 49 (1994) 99–103.

34. W.J. Frederick, T. Noopila and M. Hupa, Swelling of spent pulping liquor droplets during combustion, J. Pulp Paper Sci. 17 (5) (1991) 164–170.

35. M. Järvinen, R. Zevenhoven, E. Vakkilainen, M. Forssen, Black liquor devolatilization and swelling–a detailed droplet model and experimental validation, Biomass and Bioenergy 24 (2003) 495–509.

36. W.J. Frederick, Combustion processes in black liquor recovery: analysis and interpretation of combustion rate data and an engineering model, DOE Report DOE/CE/40637-T8, USA, 1990.

37. A.F. Mills, Heat Transfer, 2nd Edition, Prentice Hall, Upper Saddle River, NJ, 1999.

38. J. Li and A.R.P. van Heiningen, Kinetics of CO_2 gasification of fast pyrolysis black liquor char, Ind. Eng. Chem. Res. 29 (9) (1990) 1776–1785.

39. J. Li and A.R.P. van Heiningen, Kinetics of gasification of black liquor char by steam, Ind. Eng. Chem. Res. 30 (7) (1991) 1594–1601.

40. K.J. Wåg, W.J. Frederick, V. Sricharoenchaikul, T.M. Grace, M. Kymäläinen, Sulfate reduction and carbon removal during kraft char burning, Proc. 1995 Int'l Chemical Recovery Conf., pp. B35–B50.

41. C.L. Verrill, T.M. Grace, and K.M. Nichols, The significance of sodium Release during devolatilization on fume formation in kraft recovery furnaces, J. Pulp Paper Sci. 20 (12) (1994) 354–360.

42. A. Borg, A. Teder, and B. Warnqvist, Inside a kraft recovery furnace – studies on the origins of sulfur and sodium emission, Tappi J. 57 (1) (1974) 126–129.

43. J.H. Cameron, Vaporization from alkali carbonate melts with reference to the kraft recovery furnace, J. Pulp Paper Sci. 14 (4) (1988) 76–81.

44. R. Backman, B.-J. Skrifvars, M. Hupa, P Siiskonen and J. Mäntyniemi, Flue gas and dust chemistry in recovery boilers with high levels of chlorines and potassium, J. Pulp Paper Sci. 22 (4) (1996) 119–126.

45. J. Li and A.R.P. van Heiningen, Sodium emission during pyrolysis and gasification of black liquor char, Tappi J. 73 (12) (1990) 213–219.

46. E.I. Kauppinen, M.P. Mikkanen, T. Valmari, S.A. Sinquefield, W.J. Frederick, M. Hupa, R. Backman, M. Forssén, P. McKeough, V. Arpiainen, M. Kurkela, M. Moisio, J. Keskinen, and M. Mäkinen, Sodium release during black liquor pyrolysis: differences between the results from various laboratory scale experiments, Proc. 1995 Int'l Recovery Conf., Toronto, pp. 105–112.

47. A.D. Volkov, O.D. Evseev, R.I. Ibatullina, and E.I. Dravolina, Sodium loss during burning of moist particles of black liquor, Mezhuz. Sb.Naauchn. Tr. Ser. Khim. Tecknol. Tsellyul, 7 (1980) 72–75.

48. W.J. Frederick and M. Hupa, Evidence of sodium fuming during pyrolysis of black liquor, Tappi J. 74 (11) (1991) 192–194.

49. S.H. Kochesfahani, H. Tran, A.K. Jones, T.M. Grace, S.J. Lien, W. Schmidl, Particulate formation during black liquor char bed burning, J. Pulp Paper Sci. 26 (5) (2000) 180–187.

50. D.C. Dayton and W.J. Frederick, Direct observation of alkali vapor release during biomass combustion and gasification. 2. Black liquor combustion at 1100ºC, Energy Fuels 10 (1996) 284–292.

51. V.V Reis, W.J. Frederick, K.J. Wåg, K. Iisa, and S.A Sinquefield, Effects of temperature and oxygen concentration on potassium and chloride enrichment during black-liquor combustion, Tappi J. 78 (12) (1995) 67–76.

52. T. Tamminen, T. Laurén, K. Janka, and M. Hupa, Dust and flue gas chemistry during rapid changes in the operation of black liquor recovery boilers: Part 2–Dust composition, Tappi J. 1 (5) (2002) 25–29.

53. T. Tamminen, J. Kiuru, R. Kiuru, K. Janka, and M. Hupa, Dust and flue gas chemistry during rapid changes in the operation of black liquor recovery boilers: Part 1–Dust formation, Tappi J. 1 (6) (2002) 27–31.

54. L. Pejryd and M. Hupa, Bed and furnace gas composition in recovery boilers–advanced equilibrium calculations, 1984 TAPPI Pulping Conference, San Francisco, pp. 579–590.

55. W.L. Saw, M. Hupa, PJ. Ashman, G.J. Nathan, M. Forssén, Z.T. Alwahabi, Insight into the fate of atomic sodium from black liquor combustion in a flat flame using equilibrium calculations, Proc. Aust. Combust. Inst. (2007), pp. 118–121.

56. G. P. Smith, D.M. Golden, M. Frenklach, N.W. Morinarty, B. Eiteneer, M. Goldenberg, C.T. Bowman, R.K. Hanson, S. Song, W.C. Gardiner Jr., V.V. Lissianski, and Z. Qin, GRI-Mech v3.0, http://www.me.berkeley.edu/gri_mech/.

57. P Glarborg, and P. Marshall, Mechanism and modelling of the formation of gaseous alkali sulfates, Combust. Flame 141 (2005) 22–39.

58. M.U. Alzueta, R. Bilbao and P. Glarborg, Inhibition and sensitization of fuel oxidation by SO_2, Combust. Flame 127 (2001) 2234–2251.

59. K. Schofield and M. Steinberg, Sodium/sulfur chemical behavior in fuel-rich and -lean flames, J. Phys. Chem. 96 (1992) 715–726.

60. H.A. Becker, H .C. Hottel, and G.C. Williams, The nozzle-fluid concentration field of the round, turbulent, free jet, J. Fluid Mech. 20 (1967) 285–303.

61. J. Janson, O. Pekkala, The use of unconventional alkali in cooking and bleaching. Part 2. Alkali cooking of wood with the use of borate, Paperi. Puu 59 (6–7) (1977) 546–557.

62. J. Janson, The use of unconventional alkali in cooking and bleaching. Part 5. Autocausticizing reactions, Paperi. Puu 61 (1) (1979) 20–30.

63. T.M. Grace, An evolution of non-conventional causticizing technology for kraft chemical recovery (Project 3473-3), report one, A progress report to members of the institute of paper chemistry, 1981, The Institute of Paper Chemistry: Appleton, Wisconsin. pp. 1–66.

64. H.N. Tran, X. Mao, J. Cameron, and C.M. Bair, Autocausticizing recovery boiler smelt with sodium borate, Pulp Pap. Can. 100 (9) (1999) 35–40.

65. H. Tran, X. Mao, N. Lesmana, S. Kochesfahani, C. Bair, and R. McBroom, Effect of partial borate autocausticizing on kraft recovery operations, Pulp Pap. Can. 103 (12) (2002) 74–78.

66. H. Tran, C. Bair, R. McBroom, W. Strang, and B. Morgan, Partial autocausticizing of kraft smelt with sodium borates – Part 1: effects on recovery boiler performance, Tappi J. 1 (1) (2001) 1–16.

67. M. Björk, T. Sjögren, T. Lundin, H. Rickards, and S. Kochesfahani, Partial borate autocausticizing trial increases capacity at Swedish mill, Tappi J. 4 (9) (2005) 15–19.

68. M. Hupa, M. Forssén, R. Backman, A. Stubbs, and R. Bolton, Fire behaviour of black liquors containing boron, Tappi J. 1 (1) (2002) 48–52.

69. M. Ellis and S. Kochesfahani, Partial borate autocausticizing technology mill trial experiences, 2005 Tappi Engineering, Pulping, Environment Conference, pp. 20–33.

70. B.L. Chadwick, R.A. Ashman, A. Campisi, G.J. Crofts, P.D. Godfrey, P.G. Griffin, A.L. Ottrey, R.J.S Morrison, Development of techniques for monitoring gas-phase sodium species formed during coal combustion and gasification, International Journal of Coal Geology 32 (1996) 241–253.

71. F. Greger, K.T. Hartinger, P.B. Monkhouse, J. Wolfrum, H. Baumann, B. Bonn, In situ alkali concentration measurements in a pressurized, fluidised-bed coal combustor by excimer laser induced fragmentation fluorescence, Proc. Combust. Inst. 26 (1996) 3301–3307.

72. U. Gottwald, P. Monkhouse, B. Bonn, Dependence of alkali emissions in PFB combustion on coal composition, Fuel 80 (2001) 1893–1899.

73. U. Gottwald, P. Monkhouse, N. Wulgaris, B. Bonn, In-situ study of the effect of operating conditions and additives on alkali emissions in fluidised bed combustion, Fuel Proc. Tech. 75 (2002) 215–226.

74. P.B. Monkhouse, U.A. Gottwald, K.O. Davidsson, B. Lönn, K. Engvall, J.B.C. Pettersson, Phase discrimination of alkali species in PCFB combustion flue gas using simultaneous monitoring by surface ionisation and photofragmentation fluorescence, Fuel 82 (2003) 365–371.

75. M.P. Glazer, N.A. Khan, W. de Jong, H. Spliethoff, H. Schürmann, P. Monkhouse, Alkali metals in circulating fluidized bed combustion of biomass and coal: Measurements and chemical equilibrium analysis, Energy Fuels 19 (2005) 1889–1897.

76. H. Schürmann, P. Monkhouse, S. Unterberger, K.R.G. Hein, In situ parametric study of alkali release in pulverized coal combustion: Effects of operating conditions and gas composition, Proc. Combust. Inst. 31 (2007) 1913–1920.

77. V. Häyrinen, R. Hernberg, Alkali measurements using plasma excited alkali resonance line spectroscopy. In: E. Scmidt, P. Gäng, T. Piltz, A. Dittler, Editors, High temperature gas cleaning, Universität Karlsruhe, Karlsruhe (1996), pp. 694–705.

78. V. Häyrinen, R. Hernberg, M. Aho, Demonstration of plasma excited atomic resonance line spectroscopy for on-line measurements of alkali metals in a 20 kW bubbling fluidized bed, Fuel 83 (2004) 791–797.

79. P.G. Sweeney, H.B. Abrahamson, L.J. Radonovich, T.A. Ballintine, Determination of atomic sodium in coal combustion using laser-induced fluorescence, ACS Division of Fuel Chemistry, Preprints, 32 (4) (1987) 186–192a.

80. P.J. van Eyk, P.J. Ashman, Z.T. Alwahabi, G.J. Nathan, Quantitative measurement of atomic sodium in the plume of a single burning coal particle, Combust. Flame 155 (2008) 529–537.

81. L.G. Blevins, C.R. Shaddix, S.M. Sickafoose, P. M. Walsh, Laser-induced breakdown spectroscopy at high temperatures in industrial boilers and furnaces, Appl. Opt. 2003, 42, (30), 6107-6118.

82. A. Molina, P.M. Walsh, C.R. Shaddix, S.M. Sickafoose, L.G. Blevins, Laser-induced breakdown spectroscopy of alkali metals in high-temperature gas, Appl. Opt. 2006, 45, (18), 4411-4423.

83. A.C. Eckbreth, *Laser diagnostic for combustion temperature and species*, 2nd Edition, 1996, Gordon and Breach Publishers.

84. K. Kohse-Höinghaus and J.B. Jeffries, Applied combustion diagnostics, 2002, New York, London, Taylor & Francis.

85. J.W. Daily, Laser induced fluorescence spectroscopy in flame, Prog. Energy Combust. Sci. 23 (1997) 133–199.

86. C. Schulz, V. Sick, J. Heinze, and W. Stricker, Laser-induced-fluorescence detection of nitric oxide in high-pressure flames with A-X(0,2) excitation, APPLIED OPTICS, 36 (1997) 3227–3232.

87. C. Schulz, V. Sick, Trace-LIF diagnostics: quantitative measurement of fuel concentration, temperature and fuel/air ratio in practical combustion systems, Prog. Energy Combust. Sci. 31 (2005) 75–121.

88. J.W. Daily and C. Chan, Laser-induced fluorescence measurement of sodium in flames, Combust. Flame 33 (1978) 47–53.

89. A.J. Hynes, M. Steinberg, and K. Schofield, The chemical kinetics and thermodynamics of sodium species in oxygen-rich hydrogen flames, J. Chem. Phys. 80 (1984) 2585–2597.

90. J.W. Daily, Detectability limit and uncertainty considerations for laser induced fluorescence spectroscopy in flames, Applied Optics 17 (1978) 1610–1615.

91. K.T. Hartinger, S. Nord, P.B. Monkhouse, Quenching of fluorescence from Na(3^2P) and K (4^2P) atoms following photodissociation of NaCl and KCl at 193 nm, Appl. Phys. B 64 (1997) 363–367.

92. M.Y. Choi and K.A. Jensen, Calibration and correction of laser-induced incandescence for soot volume fraction measurements, Combust. Flame 112 (1998) 485–491.

93. J. Stenberg, W.J. Frederick, S. Bostrom, R. Hernberg and M. Hupa, Pyrometric temperature measurement method and apparatus for measuring particle temperatures in hot furnaces: Application to reacting black liquor, Rev. Sci. Instrum. 67 (5) (1996) 1976–1984.

94. L.D Timothy, A.F. Sarofim and J.M. Béer, Characteristic of single particle coal combustion, Proc. Combust. Inst. 19 (1982) 1123–1130.

95. D.A. Tichenor, R.E. Mitchell, K.R. Hencken and S. Niksa, Simultaneous in situ measurement of the size, temperature and velocity of particles in a combustion environment, Proc. Combust. Inst. 20 (1984) 1213–1221.

96. A. Macek and C. Bulik, Direct measurement of char-particle temperatures in fluidized-bed combustors, Proc. Combust. Inst. 20 (1984) 1223–1230.

97. F.R.A. Jorgensen and M. Zuiderwyk, Two-colour pyrometer measurement of the temperature of individual combusting particles, J. Phys. E: Sci. Instrum. 18 (1985) 486–491.

98. R. Hernberg, J. Stenberg and B. Zethraeus, Simultaneous in situ measurement of temperature and size of burning char particles in a fluidized bed furnace by means of fiberoptic pyrometry, Combust. Flame 95 (1993) 191–205.

99. S.M. Godoy and F.C. Lockwood, Development of a two-colour infrared pyrometer for coal particle temperature measurements during devolatilisation, Fuel 77 (1998) 995–999.

100. M. Idris and U. Renz, Two colour pyrometer technique for coal particle temperature measurements in pressurised pulverised coal flame, Energy Institute, 80 (4) (2007) 185–191.

101. P.J. van Eyk, P.J. Ashman, Z.T. Alwahabi and G.J. Nathan, Simultaneous measurements of the release of atomic sodium, particle diameter and particle temperature for a single burning coal particle, Proc. Combust. Inst. 32 (2009) 2099–2106.
102. W.L. Flower, Optical measurement of soot formation in premixed flames, Combustion Sci. Technol. 33 (1983) 17–33.
103. S. di Stasio and P. Massoli, Influence of the soot property uncertainties in temperature and volume-fraction measurements by two-colour pyrometry, Meas. Sci. Technol. 5 (1994) 1453–1465.
104. T. Joustsenoja, P. Heino, R. Hernberg and B. Bonn, Pyrometric temperature and size measurements of burning coal particles in a fluidized bed combustion reactor, Combust. Flame 118 (1999) 707–717.
105. T.P Jenkins and R.K. Hanson, Soot Pyrometry using modulated absorption/emission, Combust. Flame 126 (2001) 1669–1679.
106. H.C. Hottel and F.P. Broughton, Determination of true temperature and total radiation from luminous gas flames, Industrial Eng. Chem. (Anal. Ed.) 4 (2) (1932) 166–175.
107. Y. Huang, Y. Yan and G. Riley, Vision-based measurement of temperature distribution in a 500-kW model furnace using the two-colour method, Measurement 28 (2000) 175–183.
108. W.J. Frederick, M. Hupa, J. Stenberg and R. Herberg, Optical pyrometric measurements of surface temperatures during black liquor char burning and gasification, Fuel 73 (1994)1889–1893.
109. L.T. Ip, L.L. Baxter, A.J. Mackrory and D.R. Tree, Surface temperature and time-dependent measurements of black liquor droplet combustion, AIChE 54 (2008) 1926–1931.

Chapter 3

Assessment of the Release of Atomic Na from a Burning Black Liquor Droplet Using Quantitative PLIF

W.L. Saw [a], G.J. Nathan [a], P.J. Ashman [b], and Z.T. Alwahabi [b]

[a]Centre for Energy Technology, School of Mechanical Engineering, The University of Adelaide, SA 5005 Australia

[b]Centre for Energy Technology, School of Chemical Engineering, The University of Adelaide, SA 5005 Australia

Combustion and Flame 156 (2009) 1471–1479

Statement of Authorship

Assessment of the Release of Atomic Na from a Burning Black Liquor Droplet Using Quantitative PLIF

Combustion and Flame 156 (2009) 1471–1479

SAW, W.L. (Candidate)

I was responsible for the development of the measurement technique under the principal supervision of Prof. Nathan. I was also responsible for the development of the analytical model under the joint supervision of Prof. Nathan and Dr. Ashman. I performed the measurements and data processing, wrote the first draft of the manuscript and incorporated and addressed all comments and suggestions by other authors in subsequent revisions of the manuscript. Interpretation of the data was my responsibility.

I hereby certify that the statement of contribution is accurate.

Signed Date

NATHAN, G.J.

I was principal supervisor for the development of work, contributed to both data interpretation and refining of the manuscript.

I hereby certify that the statement of contribution is accurate and I have given written permission for this paper to be included in this thesis.

Signed _____ Date_____

ASHMAN, P.J.

I jointly supervised the development of work, contributed to both data interpretation and refining of the manuscript.

I hereby certify that the statement of contribution is accurate and I have given written permission for this paper to be included in this thesis.

Signed _____ Date_____

ALWAHABI, Z.T.

I, co-supervisor, was responsible for setting up and aligning the laser equipment and jointly contributed to refining of the manuscript.

I hereby certify that the statement of contribution is accurate and I have given written permission for this paper to be included in this thesis.

Signed _____ Date_____

Saw, W.L., Nathan, G.J., Ashman, P.J. & Alwahabi, Z.T. (2009) Assessment of the release of atomic Na from a burning black liquor droplet using quantitative PLIF. *Combustion and Flame, v. 156(7), pp. 1471-1479*

Chapter 4

Simultaneous Measurement of the Surface Temperature and the Release of Atomic Sodium from a Burning Black Liquor Droplet

W.L. Saw [a,b], G.J. Nathan [a,b], P.J. Ashman [a,c], Z.T. Alwahabi [a,c], and M. Hupa [d]

[a]Centre for Energy Technology, The University of Adelaide, SA 5005 Australia

[b]School of Mechanical Engineering, The University of Adelaide, SA 5005 Australia

[c]School of Chemical Engineering, The University of Adelaide, SA 5005 Australia

[d]Process Chemistry Centre, Åbo Akademi Biskopsgatan 8, FI-20500 Åbo, Finland

Revised version submitted to Combustion and Flame on 10th November 2009

Statement of Authorship

Simultaneous Measurement of the Surface Temperature and the Release of Atomic Sodium from a Burning Black Liquor Droplet

Revised version submitted to Combustion and Flame on 10th November 2009

SAW, W.L. (Candidate)

I was responsible for the development of the two-dimensional two-colour optical pyrometry technique under the principle supervision of Prof. Nathan. I performed the measurements and data processing, wrote the first draft of the manuscript and incorporated and addressed all comments and suggestions by other authors in subsequent revisions of the manuscript. Interpretation of the data was my responsibility.

I hereby certify that the statement of contribution is accurate.

Signed Date

NATHAN, G.J.

I was principal supervisor for the development of work, contributed to both data interpretation and refining of the manuscript.

I hereby certify that the statement of contribution is accurate and I have given written permission for this paper to be included in this thesis.

Signed _____ Date_____

ASHMAN, P.J.

I jointly contributed to both data interpretation and refining of the manuscript.

I hereby certify that the statement of contribution is accurate and I have given written permission for this paper to be included in this thesis.

Signed _____ Date_____

ALWAHABI, Z.T.

I jointly contributed to refining of the manuscript.

I hereby certify that the statement of contribution is accurate and I have given written permission for this paper to be included in this thesis.

Signed _____ Date_____

HUPA, M.

I jointly contributed to refining of the manuscript.

I hereby certify that the statement of contribution is accurate and I have given written permission for this paper to be included in this thesis.

Signed _____ Date_____

Title: Simultaneous measurement of the surface temperature and the release of atomic sodium from a burning black liquor droplet

Authors: Woei L. Saw [a,b], Graham J. Nathan [a,b], Peter J. Ashman [a,c], Zeyad T. Alwahabi [a,c], Mikko Hupa [d]

Affiliations: [a]**Centre for Energy Technology, The University of Adelaide, SA 5005 Australia**
[b]**School of Mechanical Engineering, The University of Adelaide, SA 5005 Australia**
[c]**School of Chemical Engineering, The University of Adelaide, SA 5005 Australia**
[d]**Process Chemistry Centre Åbo Akademi University, Biskopsgatan 8, FI-20500 Åbo, Finland**

Type of article: Full-length article

Corresponding Author: Mr. Woei L Saw
School of Mechanical Engineering
The University of Adelaide
SA 5005
Australia

Telephone: +61 8 8303 3177
Facsimile: +61 8 8303 4367
Email: woei.saw@adelaide.edu.au

Abstract

Simultaneous measurement of the concentration of released atomic sodium, swelling, surface and internal temperature of a burning black liquor droplet under a fuel lean and rich condition has been demonstrated. Two-dimensional two-colour optical pyrometry was employed to determine the distribution of surface temperature and swelling of a burning black liquor droplet while planar laser-induced fluorescence (PLIF) was used to assess the temporal release of atomic sodium. The key findings of these studies are: (i) the concentration of atomic sodium released during the drying and devolatilisation stages was found to be correlated with the external surface area; and (ii) the insignificant presence of atomic sodium during the char consumption stage shows that sodium release is suppressed by the lower temperature and by the high CO_2 contents in and around the particle.

Keywords: Black liquor; Surface temperature; Sodium; LIF

1. Introduction

Black liquor is a complex and important source of renewable fuel in the pulp and paper industry. It consists of both organic components of wood, mainly lignin, and inorganic components derived from sodium based pulping chemicals. The sodium can be bound to both organic and inorganic compounds [1]. During black liquor combustion the organically bound sodium, which is associated with the phenolic hydroxyl and carboxyl compounds, decomposes and converts to Na_2CO_3 [1]. This has been found to occur primarily in during the devolatilisation stage of black liquor combustion [3]. The purpose of burning black liquor in a kraft recovery boiler is to recover both the pulping chemicals and the heat generated from the black liquor combustion, which is converted to electricity to power the pulp mill through a steam turbine. The black liquor is sprayed into a recovery boiler, typically as droplets from 0.5–5 mm in diameter [4]. Combustion of a single droplet of black liquor can be divided into the four stages of drying, devolatilisation, char combustion and smelt oxidation [5]. Black liquor swells significantly during the devolatilisation stage, by 10–60 times in volume [6], due to gas evolution within the highly viscous droplet [4]. The drying and devolatilisation stages of combustion may overlap due to large temperature gradients within the swollen droplet (Biot number > 1) [4, 7]. During the char combustion stage char is oxidised by reaction with H_2O, CO_2, and O_2 [4] and by the reduction of Na_2CO_3 [3] and Na_2SO_4 [8]. A molten bead of smelt, consisting of inorganic components (mainly Na_2CO_3 and Na_2S), is formed at the end of the char combustion stage and the oxidation of Na_2S can occur if O_2 is available [1]. Details of the black liquor combustion by measuring swelling and surface temperature simultaneously at each stage of the combustion are required to provide an insight to support the development of reliable models.

Black liquor consists of approximately 20 wt% (dry) sodium of which approximately 8% will be released during combustion [4]. When it is fired into the recovery boiler, about 40-60% of the sodium is associated with dissolved organics. During the devolatilisation stage of black liquor combustion and gasification, carbonate is formed to balance the charge of sodium and potassium [2–3]. Measurements of fume in two kraft recovery boilers in Finland showed that 90-95% of the fume originates from burning black liquor droplets in flight and only 5-10% originates from the char bed reactions [9]. The released sodium vapours react with the combustion gases (e.g. CO_2 and SO_2) to form fume, which consists mainly of Na_2CO_3 and Na_2SO_4.

The release of sodium can occur by the physical ejection of intermediate-sized particulate matter during the devolatilisation stage [10], vaporisation of NaCl and perhaps NaOH during the devolatilisation and char combustion stages [11], reduction of Na_2CO_3 to gaseous sodium and CO_x [3] and the oxidation of Na_2S during the smelt oxidation stage [12]. While NaOH has been measured in black liquor combustion products [11–13], it is not clear whether it is vaporised from the black liquor or formed from the reaction of atomic sodium with water vapour. Experiments with NaOH salt added to Na_2CO_3–Na_2S salt mixtures resulted in only a small change in fume formation indicating that NaOH volatilisation is not a significant source of fume from black liquor combustion [12]. Sodium chloride accounts for part of the sodium release but it is not the major source of fume because the concentration of chlorides is small relative to the amount of sodium [11]. Measurements of fume formation from black liquor during pyrolysis and gasification showed clearly that sodium release during experimental tests under inert or gasification conditions was primarily due to reduction of Na_2CO_3 [3]. Under oxidising conditions with the smelt, fume formation from the oxidation of Na_2S to Na_2SO_4 with reduction of Na_2CO_3 can be a significant source of fume [14], but will occur during smelt oxidation rather than devolatilisation or char burning. Thus, the reduction of Na_2CO_3 will be the primary source of fume during kraft black liquor combustion. Possible reactions include reduction with char, H_2 and CO, though CO was found to have only a very small affect on fume formation from a Na_2CO_3–Na_2S salt mixture [3, 14].

The release of the alkali metals, chlorines and sulphur compounds from black liquor is influenced by particle temperature [15]. The increase particle temperature is the result of combustion involving homogeneous and heterogeneous reactions, heat and mass transfer, and two-phase fluid flow [16–17]. Therefore, the temperature of a burning black liquor droplet is an important parameter for a better understanding of the phenomenon, and in the development of a recovery boiler model. Simultaneous measurement of the release of atomic sodium and surface temperature is required to support the development of models and so to optimise the complex processes of fume formation. Swelling in black liquor combustion is significant [6] and its measurement is needed due to the variability in drop-to-drop swelling, which affects surface area, surface temperature and so can be expected to influence also the release of atomic sodium.

Two-colour optical pyrometry has been well-established and widely used to measure the surface temperature at a single point on burning particle(s), mainly for coal [16–23], but also to

measure soot temperature [24–27] and flame temperature [28–29]. The technique was further improved by Stenberg et al. [15] to measure the surface temperature of a burning black liquor droplet in a hot, radiating environment. It was then adapted by Frederick et al. [30] to study the influence of oxygen on the surface temperatures of a burning black liquor particle, again at a single point. Increasing the oxygen concentration in a N_2/O_2 gaseous environment increases the surface temperature of the droplet during the char combustion stage. At lower oxygen concentrations, the surface temperature of the droplet during the char combustion stage was found to be constant [30]. However, the average surface temperature was found to reach as high as 300ºC above the furnace temperature for droplets burned in air [30]. Later, the swelling, mass loss and the surface and internal temperatures of a burning black liquor droplet were measured simultaneously by Ip et al. [31]. A digital video camera fitted with two infra-red filters was used to measure the surface temperature by detecting the radiation emitted from the burning black liquor droplet at two wavelengths. This technique requires the grey emissivity (ε) of the droplet to be assumed. Nevertheless, it provided two-dimensional imaging of the surface temperature of a burning black liquor droplet. A non-uniform distribution of the surface temperature of the burning droplet was observed, along with a large temperature difference between the surface and internal temperatures throughout the combustion stages. However, no statistical information of the distribution of the surface temperature during the black liquor combustion is available at low oxygen concentration and reducing conditions (e.g. by the use of probability density functions, PDFs).

Recently, a two-dimensional, quantitative measurement of the release of high concentration atomic sodium (in the order of 1 ppm) from a burning black liquor droplet in a flat flame was conducted by Saw et al. [32] using simultaneous planar laser-induced fluorescence (PLIF) and absorption. A first-order equilibrium model was also developed in that study [32] to provide insight into the of distribution of sodium species using a Plug Flow Reactor model of CHEMKIN 4.1, based on the independently measured concentration of residual sodium in the smelt as a function of time [32]. As expected, the major sodium species calculated with the model were atomic sodium and NaOH and no Na_2CO_3 or Na_2SO_4 were identified in that model. The flat flame burner has improved optical access for the PLIF technique over a closed furnace. However, no comparison has previously been made of the difference between combustion in a flat flame with that in a furnace for black liquor. Furthermore, simultaneous measurements of sodium concentration and droplet surface temperature within a flat flame environment at either fuel-rich or fuel lean conditions have not been previously reported. The

increase of oxygen concentration within the surrounding atmosphere increases the surface temperature of the droplet [30], as described above. Hence, the increase of surface temperature may increase the release rate of atomic sodium during the combustion.

Given the absence of any simultaneous reports of the relationship between sodium release and particle temperature, the aims of the present investigation are: i) to measure the simultaneous release of atomic sodium, surface temperature and swelling as a function of time under fuel-rich and fuel-lean conditions; ii) to assess the influence of surface temperature on the release of atomic sodium; and iii) to compare the influence of the oxygen concentrations on the surface temperature in a flat flame with that in a closed furnace environment.

2. Experimental Techniques

A sample of black liquor obtained from a Swedish pulp mill, shown in Table 1, was used for the measurements. A consistent quantity droplet of black liquor (10 mg) was carefully applied to a 0.5 mm diameter Type-R (Pt/Pt-13% Rh) thermocouple, to measure its internal temperature, T_{tc}, and both were placed on a loop (3 mm diameter) at the tip of a platinum wire (0.5 mm diameter). The loop, with the thermocouple and the black liquor droplet was placed 10 mm $\pm$ 1 mm above the tip of a flat flame burner, using a retort stand. The black liquor was burned in the flame provided by the flat flame burner at two flame conditions, fuel lean ($Ø_{bg}$ = 0.8), and fuel rich ($Ø_{bg}$ = 1.25). Here the symbol $Ø_{bg}$ denotes the equivalence ratio of the burner gases alone, which were held constant throughout a given experiment, and ignores the contribution of the black liquor droplet to the fuel, which varies throughout the experiment. The flat flame burner comprised a matrix of small diffusion flames with the total burner having dimensions of 80 mm × 100 mm. Details of the burner are described elsewhere [22]. The burner was fed with local natural gas as the fuel and the compressed air was supplied by our laboratory compressor. The total flow rate of fuel and air to the burner was 65.8 *l*/min (STP). A co-flow of air was supplied around the flat flame burner to stabilize the flame from flicker. The composition of the combustion products, O_2, H_2O, CO_2 and CO, from the gas burner for both stoichiometries was calculated using the Pre-Mixed Burner model in CHEMKIN 4.1with GRI-Mech v3.0 [33] as is shown in Table 2.

The laser and optical arrangement in the present study is similar to that in Ref. [32]. Two-dimensional images were obtained using simultaneous PLIF and absorption, corrected for fluorescence trapping, with the arrangement shown in Fig. 1. The effects of collisional quenching due to collisions with major species in the flame were also incorporated into the correction. A tuneable dye laser (Lambda Physik, Scanmate), pumped by a Nd: YAG laser (Quantel, Brilliant b). The dye laser was scanned around 588–590 nm to excite the D_1 and D_2 sodium lines at 589.59 nm and 589 nm, respectively. All the measurements were performed using the D_1 line because of the strong beam absorption observed with the D_2 line. The pulse-to-pulse energy variation was measured to be about 12%. The output radiation was directed to appropriate cylindrical lenses to form a sheet of light (40 mm × 3 mm) through the flat flame, located between two glass cells containing fluorescent dye. The PLIF signal from the sodium atoms was collected using a gated intensified CCD camera (Princeton Instruments ICCD-576) aligned orthogonal to the laser sheet. A gate width of 10 ns was selected to minimise noise and background radiation from the flame. Images were recorded at five images per second. A polariser was placed in the front of the ICCD camera lens to minimize any elastic laser scattering processes. No signal was observed when the polarisation axis of the polariser was set perpendicular to the laser polarisation axis when the dye laser is tuned away from the absorption line of sodium. For absorption measurements, the incoming and outgoing laser intensity was obtained from the two dye cells calibrated for laser intensity. Measurements were taken about 15 mm above the black liquor droplet to avoid the scattered light from the particle and the platinum wire.

Three temperatures were measured in the present investigation, namely the gas flame temperature of the burner gases, T_{gf}, internal temperature, T_{tc}, (as described above) and surface temperature, T_s, of a burning black liquor droplet. The T_{gf} was measured at a height of 35 mm above the wire, without the black liquor, by a 0.5 mm diameter Type-R (Pt/Pt-13% Rh) thermocouple and the results for both stoichiometries are presented in Table 2. A separate measurement was performed with the droplet burning, and the presence of combustion was found to influence the gas temperature by no more than $\pm$ 20°C over the axial range $5 < Z < 40$ mm, where Z is the height above the wire. The measurement of T_{gf} was corrected for radiation losses from the thermocouple using the radiation correction equation of Brohez et al. [34]. The correction was typically 300°C and the uncertainties were calculated to be $\pm$ 50ºC.

The T_s measurement was determined by the two-colour pyrometry technique. This technique measures the relative emission intensity at two wavelengths and relates the ratio to the temperature of the source. Wien's law approximation, as shown in Eq. (1), is selected as it relates to the emission intensity (E_λ) of a black body to the wavelength (λ) and absolute surface temperature (T_s).

$$E_{\lambda i} = -C_1 \lambda_i^{-5} \varepsilon_{\lambda i} \exp-\left(\frac{C_2}{\lambda_i T_s}\right) \quad (1)$$

where ε_λ is emissivity of the solid surface at wavelength λ_i and C_1 and C_2 are first and second Planck's constants. The relationship between T_s and the ratio of two emission intensities, $E_{\lambda 1}$ and $E_{\lambda 2}$, as shown in Eq. (2), at wavelengths, λ_1 and λ_2, respectively, is as shown in Eq. (3).

$$\frac{E_{\lambda 1}}{E_{\lambda 2}} = \frac{\varepsilon_{\lambda 1}}{\varepsilon_{\lambda 2}} \left(\frac{\lambda_2}{\lambda_1}\right)^5 \exp\left[\frac{C_2}{T_s}\left(\frac{1}{\lambda_2} - \frac{1}{\lambda_1}\right)\right] \quad (2)$$

$$T_s = \frac{-C_2\left(\frac{1}{\lambda_1} - \frac{1}{\lambda_2}\right)}{\ln\left(\frac{\varepsilon_{\lambda 1}}{\varepsilon_{\lambda 2}} \frac{\lambda_2^5}{\lambda_1^5} \Big/ \frac{E_{\lambda 1}}{E_{\lambda 2}}\right)} \quad (3)$$

The two-colour pyrometry arrangement in the present study is adapted from that of van Eyk et al. [22]. Simultaneous and synchronised images of the history of a burning black liquor droplet were obtained by each of two similar models of camera (Canon 400D). A narrow bandpass interference filter of 532.5 nm (λ_1) and 632 nm (λ_2) was placed in front of each of the camera lens, respectively. In addition, a 50/50 beam-splitter was placed in front of the cameras to achieve equal distance from each of the two cameras to the black liquor droplet as shown in Fig. 1 and an identical field of view. Two-dimensional images of the particle radiation at the two wavelengths were captured in greyscale at the shutter speed of 1 Hz. The present difference of the wavelengths of 100 nm is within the range of 20 and 120 nm used in two-colour pyrometery in previous studies [16, 19, 23, 29]. These wavelengths are sufficiently close to each other for, the ratio of corresponding spectral emissivity of the black liquor droplet, $\varepsilon_{\lambda 1}/\varepsilon_{\lambda 2}$, to be reasonably assumed to be approximately unity. Under such conditions, the differences between the spectral emissivities of the droplet are negligible [29] and minimise the effects of any sudden variation in the absorption spectra of the gases [19]. A calibration of the ratio $E_{532.5}/E_{632}$ as a function of temperature was required due to the dependence of the intensities collected by each camera on the response of each CCD array to wavelength and the transmission through each interference filter [22]. The calibration was obtained from the average ratio of the radiation emitted from the two instantaneous

images at the bead of a thermocouple in the flame environment. The thermocouple surface temperature T_{gf}, was calibrated over the range 940–1350°C. This range of temperature was used to obtain a linear relationship for the value of $E_{532.5}/E_{632}$ from Eq. (3). The uncertainty of T_s as obtained using Eq. (3) relative to the thermocouple temperature measurement was calculated to be $\pm$ 3% ($\pm$ 30°C). For each instantaneous image (from both cameras), the edges of the burning black liquor droplet were carefully selected, since the shape of the droplet varies with time, so that each image obtained at 532.5 nm matches that at 632 nm. The T_s of the droplet was then measured for each pixel within the droplet at a resolution of 0.04×0.04 mm^2.

The images from the SLR cameras as described above were also used to measure the history of droplet diameter and estimate the duration of the drying, devolatilisation, char consumption and smelt coalescence stages simultaneously with the laser measurement of the atomic sodium. Note that the term 'char consumption' is used rather than 'char combustion' is described in Section 3.4. The time for the drying stage (t_0–t_1) was determined from the moment at which the burner was lit until the onset of the visible diffusion flame or soot. The devolatilisation stage (t_1–t_2) was determined from the onset of the diffusion flame until it disappeared. The char consumption time (t_2–t_3) was determined from the moment at which the diffusion flame disappeared until the time when the char particle collapsed to form a molten droplet. The T_s of the droplet during the smelt oxidation stage, however, could not be detected due to the collapse of the smelt onto the loop of the wire.

3. Results and Discussion

3.1 Surface temperature measurement

Figure 2 presents typical images of the swelling and the temporal history of the combustion of black liquor using the interference filters of 532.5 nm (Fig. 2a) and 632 nm (Fig. 2b) and the surface temperature (Fig. 2c), derived from raw images as per Eq. (3), for $Ø_{bg}$ = 0.8 obtained from the SLR cameras. As expected, the intensity of the burning droplet at $E_{532.5}$ was found to be less than that at E_{632}. While the measurement obtained from the background surrounding the particle is very noisy, as expected due to the low signal, that obtained from inside the droplet boundary is only noisy in the regions where the surface temperature is relatively cold (Fig. 2c). However, the average emittance from

the burning particle was found to be at least 5 times higher than that of the flame surrounding the particle. In addition, the surface temperature of the burning droplet is clearly distinguished.

A non-uniform surface temperature distribution was observed during the drying stage (t = 2 s), as shown in Fig. 2c-I. During the devolatilisation, similar observations of non-uniform surface temperature and also large pores near to the wire were observed (Fig. 2c-II). As expected, soot was detected during this stage at the top right of Fig. 2c-II. During the early stage of char consumption, t = 6–8 s, the variation in T_s (Figs. 2c-III and 2c-IV) was observed to be smaller than that during the devolatilisation stage (Fig. 2c-II). However, the temperature at t = 10s (Fig. 2c-V) just above the wire was found to be at least 100ºC higher than that during the devolatilisation stage. At the end of the char consumption stage (t = 12 s), all the char had collapsed to form into a smelt bead on the loop of the wire.

Figure 3 presents a scatter plot of all of the measurements of T_s on a pixel-by-pixel basis and the radial distribution of mean surface temperature, $\overline{T}_s(r)$, as function of radial location, r, at t = 6 s for $Ø_{bg}$ = 0.8 and 1.25. The distribution of T_s shown in Fig. 3a corresponds to the image as shown in Fig. 2c-III. It can be seen that there is no consistent dependence of the distribution on r and that mean variations are small. This implies that there is no advantage in correcting projected area to surface area. Furthermore, such a correction would not account for the convoluted shape of the surface, which is not realistic to correct for. Here all statistics are based on projected area, as measured on a pixel-by-pixel basis.

Figure 4 presents the mean surface temperature distribution, an average of 0.5 mm on each side (or 25 × 1 pixels) at the centreline of the droplet above the wire, $\overline{T}_s(Z)$, for both stoichiometries as a function of time. The extent of swelling in the vertical direction can also be deduced from the length of each line. For $Ø_{bg}$ = 0.8, $\overline{T}_s(Z)$ is typically greatest at the wire, and decreases sharply over the first two mm as shown in Fig. 4a. The value of $\overline{T}_s(Z)$ increases again toward the tip significantly at t = 8 and 10 s. This increase in temperature is most likely to be due to the strongly exothermic nature of the smelt oxidation reaction, where O_2 diffuses within the droplet through the large pores, as described above (Fig. 2). For $Ø_{bg}$ = 1.25, $\overline{T}_s(Z)$ is typically highest at the wire except at t = 2–4 s, and decreases significantly toward the end of the char consumption stage (t = 16–20 s) at the first 1.5 mm (Fig. 4b). The high value of $\overline{T}_s(Z)$ for $Ø_{bg}$ = 1.25 at the end of the char consumption (t = 16–20 s) could be due to

the exposure of smelt to the unburnt O_2 in the flame. The value of $\overline{T}_s(Z)$ of the droplet just above the wire and at the tip (t = 8–10 s) for $Ø_{bg}$ = 0.8 was found to be at least 100ºC higher than that for $Ø_{bg}$ = 1.25. This implies that the higher the O_2 concentration the higher $\overline{T}_s(Z)$.

3.2 The distribution of surface temperature

Figure 5 presents the normalised probability distributions of T_s of one droplet for $Ø_{bg}$ = 0.8 and another droplet for $Ø_{bg}$ =1.25. Here, $n(T_s)$, is defined as the number of pixels within each bin of ΔT = 10ºC over the range of resolution (940–1350ºC) and Σn is the total number pixels. We have defined T_s which occurs at the maximum value of $n(T_s)/\Sigma n$, for each time, t, as the most probable surface temperature, $T_{s,mod}$. A non-uniform T_s of the burning black liquor droplet were found for both stoichiometries throughout the combustion stages, as is shown in Fig. 4. This is consistent with the study of Ip et al. [31], which the non-uniform T_s ranged from 1000–1400ºC, in a closed furnace at 21% O_2. The variation of the T_s distribution for $Ø_{bg}$ = 0.8 was found to be at least 100ºC larger than that for $Ø_{bg}$ = 1.25 (Fig. 5~~6~~) due to the influence of O_2 concentration consistent with Fig. 4. The $n(T_s)/\Sigma n$ over T_s for $Ø_{bg}$ = 0.8 and 1.25 is typically positive skewed rather than Gaussian. The positive skewed distribution represents $n(T_s)/\Sigma n$ is weighted on left-hand of the figure. The range $n(T_s)/\Sigma n$ is from 940–1200ºC for $Ø_{bg}$ = 0.8 and 940–1150ºC for $Ø_{bg}$ = 1.25.

3.3 Analysis of heat transfer to droplet

An analysis of the contributions of each mode of heat transfer, radiation, $\dot{Q}_{Rad}$, convection, $\dot{Q}_{Conv}$, and conduction, $\dot{Q}_{Cond}$ to a black liquor droplet on the suspended wire for both conditions was performed and the results are shown in Fig. 6. The surface area employed to obtain $\dot{Q}_{Rad}$ and $\dot{Q}_{Conv}$ was calculated assuming the droplet to be a cylinder based on the observations of Fig. 2 and the dimensions was obtained from the SLR camera. Here, the $T_{s,mod}$ was selected as the input value of droplet surface temperature.

As expected for a flat flame environment, the sign of $\dot{Q}_{Rad}$ is positive, indicating cooling, while that of $\dot{Q}_{Conv}$ and $\dot{Q}_{Cond}$ are negative, indicating heating. During the drying stage, the $\dot{Q}_{Rad}$ for

$Ø_{bg}$ = 0.8 and 1.25 were found to be higher than the combined $\dot{Q}_{Conv}$ and $\dot{Q}_{Cond}$ by a factor of 2.8 and 2.3, respectively, as shown in Fig. 6. During the devolatilisation stage, the $\dot{Q}_{Rad}$ at for $Ø_{bg}$ = 0.8 and 1.25 was found to be higher than the combined $\dot{Q}_{Conv}$ and $\dot{Q}_{Cond}$ by a factor of 3.6 and 2.9, respectively. The dominance of $\dot{Q}_{Rad}$ is due to the large surface area resulting from the significant swelling of the droplet and the cold walls of the laboratory. During the char consumption stage, the $\dot{Q}_{Rad}$ and $\dot{Q}_{Conv}$ decrease as the swelling factor in surface area, A/A_i decreases as is shown in Fig. 7. Note that the swelling, surface area (A), is normalised by the initial surface area (A_i). The influence of the wire on $\dot{Q}_{Cond}$ was found to be most significant one second after ignition due to the large temperature difference of at least 500ºC between the wire temperature and $T_{s,mod}$. However, the influence of $\dot{Q}_{Cond}$ to the total heat transfer is insignificant due to the temperature difference between the wire and the $T_{s,mod}$ being about 100ºC for the imaging of the burn time. Overall, the positive value of $\dot{Q}_{Tot}$ for $Ø_{bg}$ = 0.8 and 1.25 indicating that the droplet was cooled by the radiation.

3.4 Simultaneous measurement

Figure 7 presents the simultaneous measurement of most probable surface temperature, $T_{s,mod}$, thermocouple temperature, T_{tc}, the swelling factor in surface area, A/A_i, and the release concentration of atomic sodium at a distance of 35 mm above the black liquor droplet, $[Na]_{35}$, for $Ø_{bg}$ = 0.8 and 1.25. Here, the T_{tc} is referred to as an internal temperature of the droplet near the wire rather the overall internal temperature. The parameter of $[Na]_{35}$ is selected for both stoichiometries because the concentration of the atomic sodium was found to be constant with axial distance at a distance of 35 mm above the droplet and this location is sufficiently far from the particle surface to be unaffected by surface reactions [32]. The solid line, as shown in Fig. 7, represents an average of five pixels (5 × 1) at the centre-line of the sodium plume.

The values of $T_{gf,35}$ for both stoichiometries were at least 500ºC higher than $T_{s,mod}$. This can be explained by the significant loss of $\dot{Q}_{Rad}$ to the wall as described above. The value of $T_{s,mod}$ was found to increase significantly from room temperature to 990ºC for $Ø_{bg}$ = 0.8 and to 960ºC for $Ø_{bg}$ = 1.25 within one second after the ignition. The value of T_{tc} was found to increase significantly from room

temperature to 500ºC for $Ø_{bg}$ = 0.8 and to 400ºC for $Ø_{bg}$ = 1.25 within two second after the ignition (Fig. 9). Note that the response time of the thermocouple was found to be 1.5 s, resulting in the magnitude of temperature gradients being under-estimated, although the trends with respect to time are accurate. Over the same period, the value of $[Na]_{35}$ increased from 0 to 0.03 ppm (Fig. 7) for $Ø_{bg}$ = 0.8 and to 0.085 ppm for $Ø_{bg}$ = 1.25. The release of atomic sodium and the high surface temperature during the drying stage was due to the overlap in the processes of devolatilisation and char consumption as a result of high gas flame temperature. This overlap is evidenced by the large A/A_i of 5 for $Ø_{bg}$ = 0.8 and 6 for $Ø_{bg}$ = 1.25 (Fig. 7) and the hot glowing regions of the droplet as can be observed from Fig. 2a.

Interestingly, the droplet shrinks by approximately 20% of the maximum swelling at the end of the drying the stage compared with that at the beginning of the devolatilisation stage for both stoichiometries as shown in Fig. 7. However, the $T_{s,mod}$ was found to increase slightly from 990 to 1000ºC for $Ø_{bg}$ = 0.8 and from 970 to 990ºC for $Ø_{bg}$ = 1.25, while T_{tc} was found to increase from 500 to 900ºC and 400 to 800ºC for $Ø_{bg}$ = 0.8 and 1.25, respectively. The $[Na]_{35}$ and A/A_i increase significantly from 0.02 ppm to 0.085 ppm and 4 to 8, respectively, for $Ø_{bg}$ = 0.8 toward the end of the devolatilisation stage as shown in Fig. 7. For $Ø_{bg}$ = 1.25, the $[Na]_{35}$ and A/A_i increase significantly from 0.085 ppm to 0.12 ppm and 5 to 10, respectively. The release of atomic sodium during the devolatilisation stage seems to be strongly correlated with the external surface area rather than the surface temperature. A release of atomic sodium during the devolatilisation stage was seen as T_{tc} increases from 400 to 900ºC, with more released at the end the devolatilisation stage (with an internal temperature ~900ºC). This is consistent with the findings of Li and van Heiningen [3] which showed that sodium carbonate is formed during the early stages of devolatilisation and then a part of the sodium carbonate is reduce, releasing sodium vapour. However, the release of atomic sodium may react instantaneously with the surrounding gases to form molecular sodium species, which cannot be detected by the PLIF. The sodium release through the physical ejection mechanism in this flat flame environment can be assumed to be negligible because the total sodium loss from the analysis of the residual was less than 1% of sodium black liquor solids BLS [32] compared with at least 10% in a closed furnace at 900°C [10].

During the char consumption stage, the T_{tc} was found to be 100°C and 200°C higher than the $T_{s,mod}$ for $Ø_{bg}$ = 0.8 and 1.25, respectively, as shown in Fig. 7. This can be explained by the significant loss of heat due to radiation ($\dot{Q}_{Rad}$) from the particle surface to the surrounding, which reduces the

droplet surface temperature due to the large surface area, as described in Section 3.3. Note that $T_{s,mod}$ is the median surface temperature within the burning droplet. Secondly, the heat conduction from the opened thermocouple wire, which is exposed to the flame, and from the thermocouple, which is located at the flame front, could increase T_{tc}. While the A/A_i decreases gradually from 8 to 1 for $Ø_{bg}$ = 0.8 and from 10 to 1 for $Ø_{bg}$ = 1.25 as the char is consumed by oxidation or gasification reactions. The value of $T_{s,mod}$ was found to be relatively constant at 1000°C at t = 4–10 s for $Ø_{bg}$ = 0.8 and at 970°C at t = 4.5–16 s for $Ø_{bg}$ = 1.25 (Fig. 7). At such high gas flame temperature (~1000ºC), film mass transfer is considered to be the rate controlling process [8]. Frederick and Hupa [4] suggested that when the combined CO_2 and H_2O concentration is twice the oxygen concentration, almost all of the O_2 is consumed in the gas boundary layer surrounding the burning particle. In the present flame conditions, the combined CO_2 and H_2O concentration for $Ø_{bg}$ = 0.8 and 1.25 was found to be at least 6 times the excess O_2, as shown in Table 2, where all the O_2 is most likely consumed in the gas boundary layer surrounding the burning particle for both the fuel-rich and fuel-lean flames [4]. Since the char is presently being consumed mainly by CO_2 and H_2O, the term 'char consumption' is used. The increase in $T_{s,mod}$ for both stoichiometries at the end of the char consumption could be due to the overlapping process of char consumption and oxidation of Na_2S with the unburnt O_2 in the flat flame. The $[Na]_{35}$ was found to increase gradually from 0.04 to 0.06 ppm for $Ø_{bg}$ = 0.8 and 0.07 to 0.11 ppm for $Ø_{bg}$ = 1.25, which was less than the peak $[Na]_{35}$ at the end of the devolatilisation.

Figure 8 presents the derivative or gradient of each of $[Na]_{35}$, A/A_i and $T_{s,mod}$ as shown in Fig. 7. The findings of the derivatives $d[Na]_{35}/dt$, $d[A/A_i]/dt$ and $dT_{s,mod}/dt$ peak during the drying stage indicate a strong surface temperature and the increase of the external surface area on the release of atomic sodium. Strong correlations between $d[Na]_{35}/dt$ and $d[A/A_i]/dt$ was detected at the end of the devolatilisation stage (Figs. 8a and 8b) for both stoichiometries. After the devolatilisation stage, there is a sharp decrease in $d[Na]_{35}/dt$ at the beginning of the char consumption, which again correlates with the drop in $d[A/A_i]/dt$ (Fig. 8b). The $d[Na]_{35}/dt$ was then found to be constant due to the inhibition of CO_2 as described above.

3.5 Comparison of the influence of oxygen on the surface temperature

Figure 9 presents a comparison of the influence of O_2 concentrations on the $T_{s,mod}$ in the flat flame and the maximum temperature, $T_{s,max}$, in a closed furnace environment. The initial mass of the black liquor droplet, the slip velocity and $T_{gf,35}$/furnace temperature ($T_{furnace}$) temperature within the furnace and in the flat flame are shown Table 2. Note that the dominant gaseous environment within the furnace was N_2, with O_2 added at concentrations of up to 15.8 and 21 vol %, respectively. During the char consumption stage, $T_{s,mod}$ was found to be relatively constant at 1000°C and 970°C for $Ø_{bg}$ = 0.8 (3.7% O_2) and 1.25 (0% O_2), respectively, consistent with Fig. 7. This is also consistent with the study of Frederick et al. [30], which the profile of the surface temperature at lower O_2 concentrations was found to be constant, as described above. Note that these temperature profiles are different from those shown in shown Fig. 9. In contrast, within the furnace (800°C), there is a clear increase of surface temperature to 920°C and 1150°C for O_2 concentrations at 15.8 and 21%, respectively, during the char combustion stage. Therefore, the significant increase of surface temperature during the char combustion stage is mainly due to the high O_2 concentrations. Interestingly, the char burnout time for $Ø_{bg}$ = 0.8 (3.7% O_2) was found to be similar in the flat flame and the furnace at 15.8% O_2 in the furnace. Further studies on the influence of high O_2 concentrations on the surface temperature in the flame will be conducted to compare that within the furnace.

3.6 The influence of oxygen on the surface temperature

The difference between $T_{s,mod}$ and $T_{gf,35}$ in the flame during the char consumption stage as a function of O_2 concentration is shown in Fig. 10. These data are compared with $T_{s,max}$ and $T_{furnace}$ of Frederick et al. [30] obtained in a closed furnace environment (Fig. 10). The error bars in that study represent the minimum and maximum temperature difference at each O_2 concentration. The surface temperatures of the burning particle based on the size particle ranged 3–14 mg were used in that study. Note that the temperature difference between $T_{s,max}$ and $T_{furnace}$ can be directly calculated but not that between $T_{s,mod}$ and $T_{gf,35}$ in the flame. This is because the value of $T_{gf,35}$ varied for each of the conditions (Table 2), and was measured to be at least 650ºC higher than $T_{s,mod}$ for all the conditions. The difference between $T_{s,mod}$ and $T_{gf,35}$ is normalised by a reference temperature difference at 0% O_2

concentration ($Ø_{bg}$ = 1.25), $(T_{s,mod} - T_{gf,35})_{ref}$, to obtain a positive value and that can be comparable with the temperature difference between $T_{s,max}$ and $T_{furnace}$. As expected, the surface temperature increases with O_2 concentration. The gradient of the temperature difference for the present study was found to be steeper by a factor of 2 than that of the previous findings. This is consistent with $T_{gf,35}$ was at least 800°C higher than the furnace temperature, which increases the overall rates of heating and reactions.

4. Conclusion

Simultaneous measurement of the release of atomic sodium, swelling, and the two-dimensional surface temperature of a burning black liquor droplet under a fuel lean and rich condition has been demonstrated for the first time. The key findings of the present investigation are:

1. The release of atomic sodium during the drying stage is mainly due to the overlapping processes of the devolatilisation and char consumption stages, which can also occur in a kraft recovery boiler;
2. The release concentration of atomic sodium during the drying and devolatilisation stages was found to be correlated with the external surface area;
3. The gasification process, endothermic reaction, is the dominant process during the char consumption due to the high concentration of H_2O and CO_2 at high gas flame temperature. The insignificant increase of surface temperature during the char consumption stage is caused by the endothermic reaction;
4. The insignificant presence of atomic sodium during the char consumption stage shows that sodium release is suppressed by the lower temperatures and by the high CO_2 content in and around the particle - consistent with a slower reduction of Na_2CO_3;
5. The influence of the O_2 concentration on the temperature difference between the surface and the surrounding temperature increases as the surrounding temperature is increased.

5. Acknowledgements

The authors would like to acknowledge Mr. Philip van Eyk, also from the School of Chemical Engineering, for his assistance in the experimental setup. Dr. Nikolai DeMartini of the Process

Chemistry Centre, Åbo Akademi University, for his valuable comments on this manuscript. Support for this study was also provided by the Faculty of Engineering, Computer and Mathematical Sciences (ECMS), The University of Adelaide, Divisional Scholarship and Australian Research Council. The anonymous reviewers of this manuscript are also gratefully acknowledged for their insight comments on this manuscript.

6. References

[1] T.M. Grace, D.G. Sachs, H.J. Grady, *TAPPI J.* 60 (4) (1977) 122–125.

[2] M. Forssén, M. Hupa, S. Kochesfahani, H. Rickards, Autocausticization by Borate in Burning Black Liquor Droplets, *Proc. 2004 Int'l Chemical Recovery Conf.*, pp. 191–199.

[3] J. Li, A.R.P. van Heiningen, *TAPPI J.* 73 (12) (1990) 213–219.

[4] Wm.J. Frederick, M. Hupa, Black liquor Droplet Burning Processes, in *Kraft Recovery Boilers*, T.N. Adams, Editor. 1997, TAPPI Press: Atlanta, Georgia, USA. pp. 131–160.

[5] M. Hupa, P. Solin, R. Hyöty, *J. Pulp Paper Sci.* 13 (2) (1987) 67–72.

[6] W.J. Frederick, T. Noopila, M. Hupa, *J. Pulp Paper Sci*. 17 (5) (1991) 164–170.

[7] W.J. Frederick, Combustion Processes in Black Liquor Recovery: Analysis and Interpretation of Combustion Rate Data and an Engineering Model, DOE Report DOE/CE/40637-T8, USA, 1990.

[8] K.J. Wåg, W.J. Frederick, V. Sricharoenchaikul, T.M. Grace, M. Kymäläinen, Sulfate reduction and carbon removal during Kraft char burning, *Proc. 1995 Intl. Chemical Recovery Conf.*, TAPPI, pp. B35–B50.

[9] T. Tamminen, J. Kiuru, R. Kiuru, K. Janka, M. Hupa, *Tappi J.* 1 (5) (2002) 27–31.

[10] C. L. Verrill, T.M. Grace, K.M. Nichols, *J. Pulp Paper Sci.* 20 (12) (1994) 354–360.

[11] D. C. Dayton, W. J. Frederick, *Energy & Fuels* 10 (1996) 284-292.

[12] J.H. Cameron, *J. Pulp Paper Sci.* 14 (4) (1988) 76–81.

[13] A. Tavares, H.N. Tran, D. Barham, P. Rouilard, B. Adams, Fume chemistry, morphology, and deposition in a kraft recovery boiler. Proc 1995 Intl. Chemical Recovery Conf., Toronto, Canada April 23-27, 1995, pp. A87–A93.

[14] J.H. Cameron, Chem. Engin. Comm. 59 (1987) 243–257.

[15] J. Stenberg, W.J. Frederick, S. Bostrom, R. Hernberg, and M. Hupa, *Rev. Sci. Instrum.* 67 (5) (1996) 1976–1984.

[16] L.D Timothy, A.F. Sarofim, J.M. Béer, *Proc. Combust. Inst.* 19 (1982) 1123–1130.

[17] D.A. Tichenor, R.E. Mitchell, K.R. Hencken, S. Niksa, *Proc. Combust. Inst.* 20 (1984) 1213–1221.

[18] A. Maček, C. Bulik, *Proc. Combust. Inst.* 20 (1984) 1223–1230.

[19] F.R.A. Jorgensen, M. Zuiderwyk, *J. Phys. E: Sci. Instrum.* 18 (1985) 486–491.

[20] R. Hernberg, J. Stenberg, B. Zethraeus, *Combust. Flame* 95 (1993) 191–205.

[21] S.M. Godoy, F.C. Lockwood, *Fuel* 77 (1998) 995–999.

[22] M. Idris, U. Renz, *Energy Institute*, 80 (4) (2007) 185–191.

[23] P.J. van Eyk, P.J. Ashman, Z.T. Alwahabi, G.J. Nathan, *Proc. Combust. Inst.* 32 (2009) 2099–2106.

[24] W.L. Flower, Combustion Sci. Technol. 33 (1983) 17–33.

[25] S. di Stasio, P. Massoli, *Meas. Sci. Technol.* 5 (1994) 1453–1465.

[26] T. Joustsenoja, P. Heino, R. Hernberg, B. Boon, *Combust. Flame* 118 (1999) 707–717.

[27] T.P Jenkins, R.K. Hanson, *Combust. Flame* 126 (2001) 1669–1679.

[28] H.C. Hottel, F.P. Broughton, *Industrial Eng. Chem. (Anal. Ed.)* 4 (2) (1932) 166–175.

[29] Y. Huang, Y. Yan, G. Riley, *Measurement* 28 (2000) 175–183.

[30] W.J. Frederick, M. Hupa, J. Stenberg, R. Herberg, *Fuel* 73 (1994)1889–1893.

[31] L.T. Ip, L.L. Baxter, A.J. Mackrory, D.R. Tree, *AIChE* 54 (2008) 1926–1931.

[32] W.L. Saw, G.J. Nathan, P.J. Ashman, Z.T. Alwahabi, *Combust. Flame* 156 (2009) 1471–1479.

[33] G.P. Smith, D.M. Golden, M. Frenklach, N.W. Morinarty, B. Eiteneer, M. Goldenberg, C.T. Bowman, R.K. Hanson, S. Song, W.C. Gardiner Jr., V.V. Lissianski, Z. Qin, GRI-Mech v3.0, http://www.me.berkeley.edu/gri_mech/

[34] S. Brohez, C. Delvosalle, G. Marlair, *Fire Safety Journal* 39 (2004) 399–411.

Table 1

The elemental composition of the black liquor, given as percentage of dry solid content, and the effective heating value of the liquor.

	Weight - % of Wet black liquor
Dry solids (DS)	74.00
Chemical analysis	Weight - % of DS
Carbon	30.30
Hydrogen	3.50
Nitrogen	0.20
Sulphur	3.74
Sodium	22.00
Potassium	1.59
Chlorine	0.05
Oxygen (by balance)	38.60
Effective heating value	10700 kJ/kg

Table 2

The initial mass of the droplet, bulk gas composition, slip velocity and the furnace temperature, $T_{furnace}$ or the gas flame temperature, $T_{gf,35}$.

	$T_{gf,35}$ (°C)	$T_{furnace}$ (°C)	Apparatus	Initial mass (mg)	$Ø_{bg}$	O_2 (vol %)	H_2O (vol %)	CO_2 (vol %)	CO (vol %)	Slip velocity (m/s)	Author
1	1725	-	Flat flame burner	10.0	1.25	0	15.5	7.9	<0.1	1.0	Present study
2	1600	-	Flat flame burner	10.0	0.8	3.7	18.5	5.7	5.3	0.8	Present study
3	-	800	Closed furnace	10.8	-	15.8	0	0	0	0	[30]
4	-	800	Closed furnace	11.0	-	21.0	0	0	0	0	[30]

FIGURE CAPTIONS

Fig. 1. The experimental apparatus used to image sodium by simultaneous measurement of PLIF and absorption technique, and temperature by the two-dimensional two-colour optical pyrometry during the combustion of a black liquor droplet.

Fig. 2. Time history of images of a burning black liquor droplet for $Ø_{bg} = 0.8$ a) raw image at 532 5 nm; b) raw image at 632 nm; and c) surface temperature derived from raw images as per Eq. (3) during (I) drying ($t = 2$ s); (II) devolatilisation ($t = 4$ s); and (III-V) char consumption ($t = 6$–10 s). White line = edge of droplet.

Fig. 3. Scatter plot, shown in square, of T_s distribution and $\overline{\boldsymbol{T}}_{\mathbf{s}}(r)$, shown in solid line, of the particle based on projected area at $t = 6$ s for a) $Ø_{bg} = 0.8$ and b) $Ø_{bg} = 1.25$.

Fig. 4. The axial distribution of mean surface temperature, $\overline{\boldsymbol{T}}_{\mathbf{s}}(Z)$, for an initial diameter, $d_o = 2.5$ mm for a) $Ø_{bg} = 0.8$ and b) $Ø_{bg} = 1.25$.

Fig. 5. Probability distribution of the T_s (solid lines) based on projected area of a burning black liquor droplet at a) $Ø_{bg} = 0.8$ and b) $Ø_{bg} = 1.25$.

Fig. 6. The analysis of the heat transfer to a black liquor droplet for a) $Ø_{bg} = 0.8$ and b) $Ø_{bg} = 1.25$. The stages of drying, devolatilisation and char consumption stages are identified in Section 2.4. Here $\dot{\boldsymbol{Q}}_{\mathbf{i}}$ = any of the heat of conduction, $\dot{\boldsymbol{Q}}_{\mathbf{Conv}}$ = heat convection, $\dot{\boldsymbol{Q}}_{\mathbf{Rad}}$ = heat radiation and $\dot{\boldsymbol{Q}}_{\mathbf{Tot}}$ = sum of all the heat components.

Fig. 7. Simultaneous measurement of $[Na]_{35}$ (solid line), A/A_i (○), $T_{s,mod}$ (□), and T_{tc} (■) at a) $Ø_{bg} = 0.8$ and b) $Ø_{bg} = 1.25$. The stages of drying, devolatilisation and char consumption stages are identified in Section 2.4.

Fig. 8. Variations of $d[Na]_{35}/dt$, $d[A/A_i]/dt$ and $dT_{s,mod}/dt$ for a) $Ø_{bg} = 0.8$ and b) $Ø_{bg} = 1.25$. The stages of drying, devolatilisation and char consumption stages are identified in Section 2.4.

Fig. 9. Comparison of the influence of O_2 concentrations in a flame and within a furnace on the surface temperature as a function of time.

Fig. 10. The influence of O_2 concentration (vol %) on the surface temperature during the char consumption/combustion (include error bars-min and max temperature)

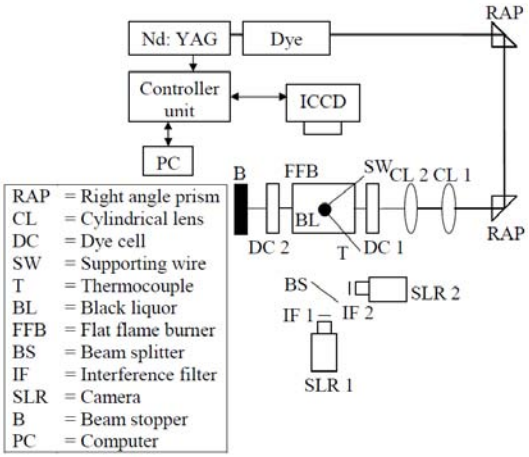
RAP
Nd: YAG
Dye
Controller unit
ICCD
PC
B
FFB
SW
CL 2
CL 1
RAP
BL
DC 2
T
DC 1
BS
SLR 2
IF 1
IF 2
SLR 1
RAP = Right angle prism
CL = Cylindrical lens
DC = Dye cell
SW = Supporting wire
T = Thermocouple
BL = Black liquor
FFB = Flat flame burner
BS = Beam splitter
IF = Interference filter
SLR = Camera
B = Beam stopper
PC = Computer

Figure 1

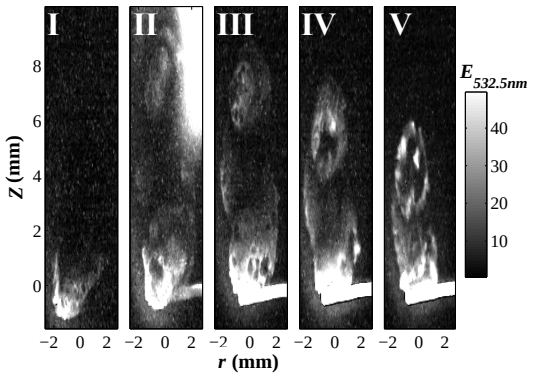
I
II
III
IV
V
Z (mm)
r (mm)
E532.5nm
40
30
20
10

a)

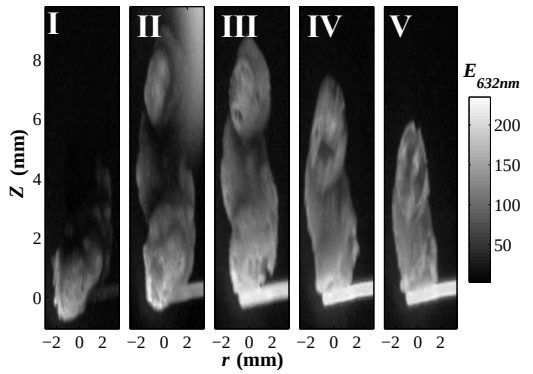
I
II
III
IV
V
Z (mm)
r (mm)
E632nm
200
150
100
50

b)

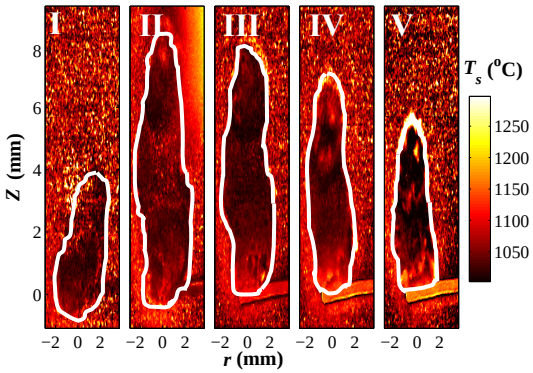
I
II
III
IV
V
Z (mm)
r (mm)
Ts (°C)
1250
1200
1150
1100
1050

c)

Figure 2

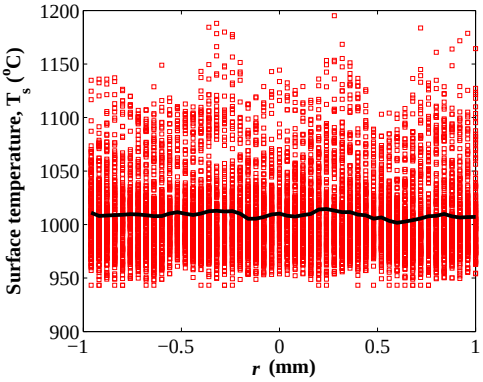
Surface temperature, T_s (^{o}C)
1200
1150
1100
1050
1000
950
900
−1
−0.5
0
0.5
1
r (mm)

a)

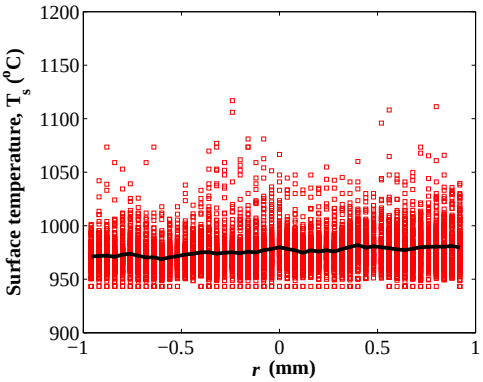
Surface temperature, T_s (^{o}C)
1200
1150
1100
1050
1000
950
900
−1
−0.5
0
0.5
1
r (mm)

b)

Figure 3

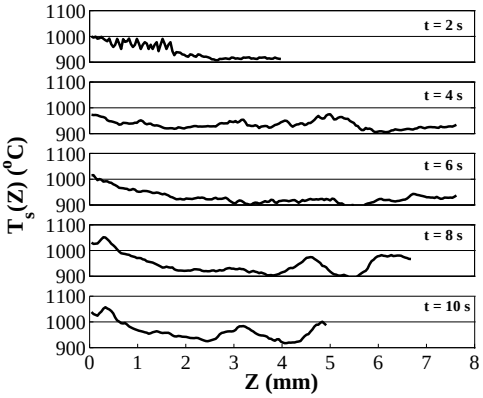
t = 2 s
t = 4 s
t = 6 s
t = 8 s
t = 10 s
T_s (Z) (^{0}C)
Z (mm)

a)

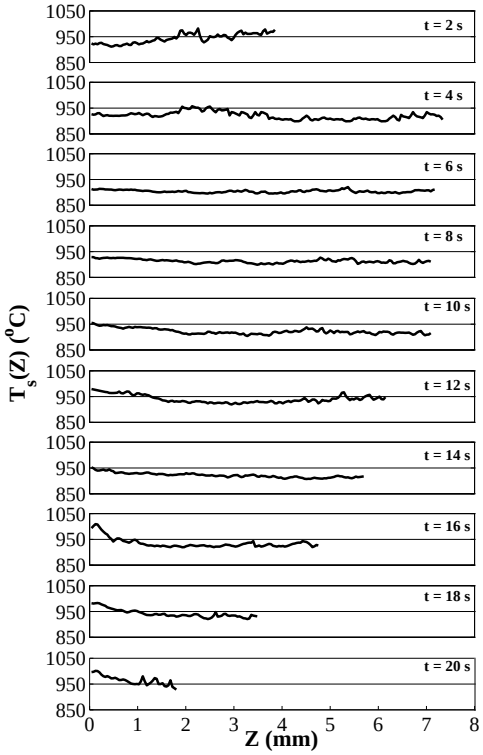
t = 2 s
t = 4 s
t = 6 s
t = 8 s
t = 10 s
t = 12 s
t = 14 s
t = 16 s
t = 18 s
t = 20 s
T_s (Z) (^{0}C)
Z (mm)

b)

Figure 4

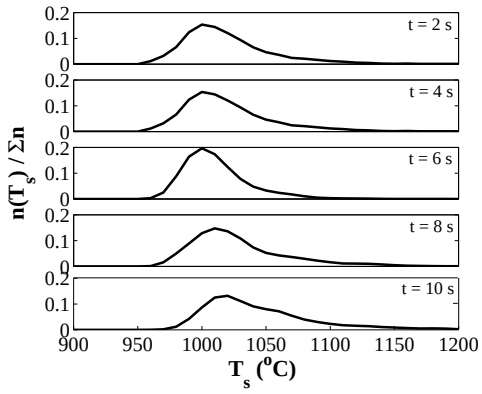
t = 2 s
t = 4 s
t = 6 s
t = 8 s
t = 10 s
0.2
0.1
0
n(T_s) / Σn
900 950 1000 1050 1100 1150 1200
T_s (°C)

a)

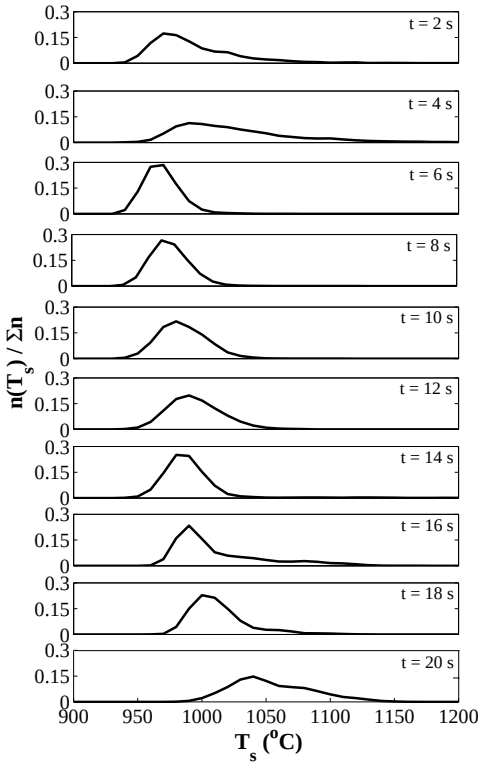
t = 2 s
t = 4 s
t = 6 s
t = 8 s
t = 10 s
t = 12 s
t = 14 s
t = 16 s
t = 18 s
t = 20 s
0.3
0.15
0
n(T_s) / Σn
900 950 1000 1050 1100 1150 1200
T_s (°C)

b)

Figure 5

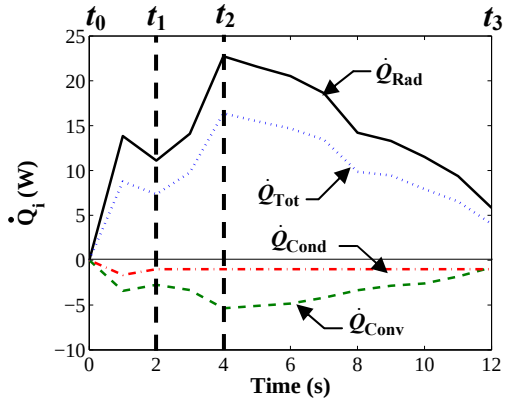
t0
t1
t2
t3
$\dot{Q}_{Rad}$
$\dot{Q}_{Tot}$
$\dot{Q}_{Cond}$
$\dot{Q}_{Conv}$
$\dot{Q}_i$ (W)
Time (s)

a)

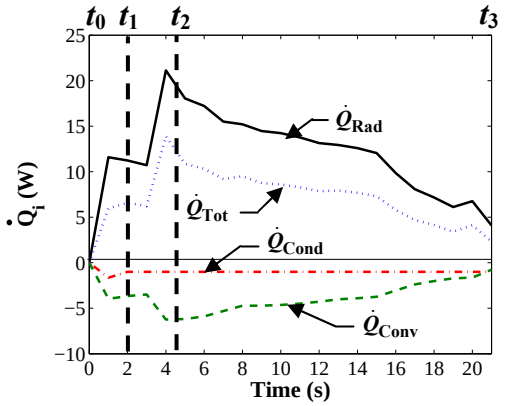
t0
t1
t2
t3
$\dot{Q}_{Rad}$
$\dot{Q}_{Tot}$
$\dot{Q}_{Cond}$
$\dot{Q}_{Conv}$
$\dot{Q}_i$ (W)
Time (s)

b)

Figure 6

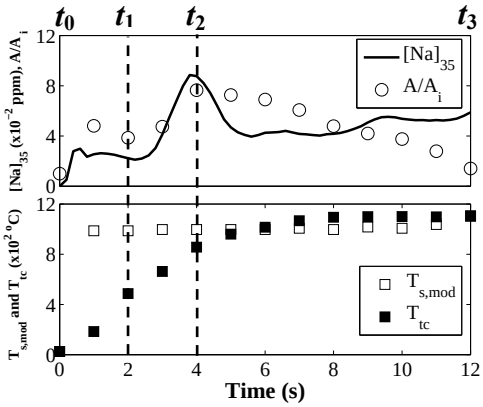

a)

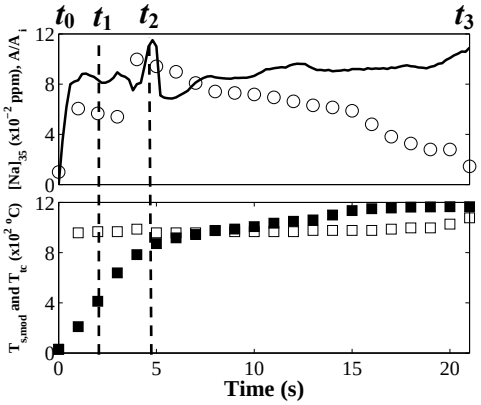

b)

Figure 7

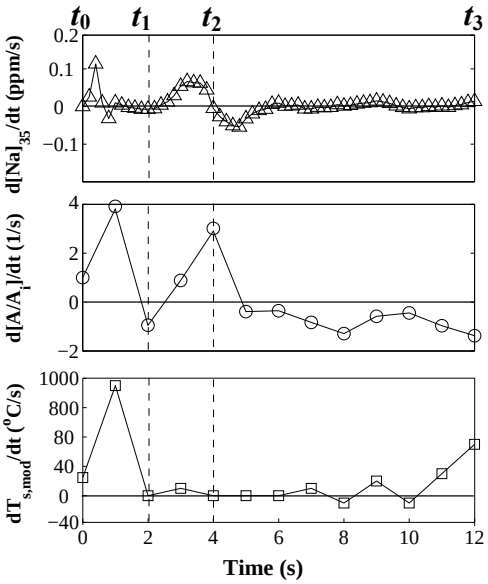
t0
t1
t2
t3
d[Na]35/dt (ppm/s)
d[A/Ai]/dt (1/s)
dTs,mod/dt (°C/s)
Time (s)

a)

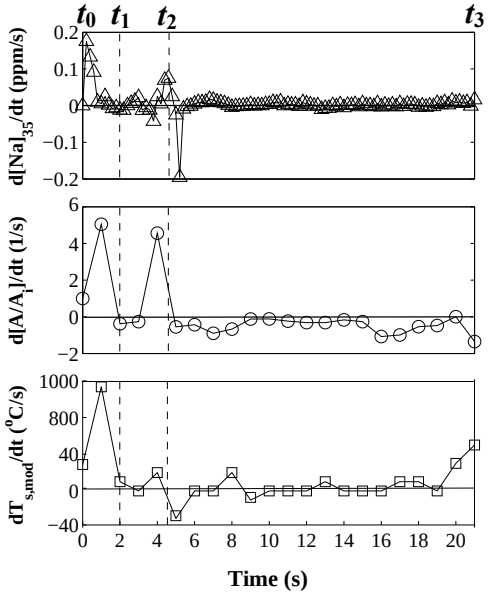
t0
t1
t2
t3
d[Na]35/dt (ppm/s)
d[A/Ai]/dt (1/s)
dTs,mod/dt (°C/s)
Time (s)

b)

Figure 8

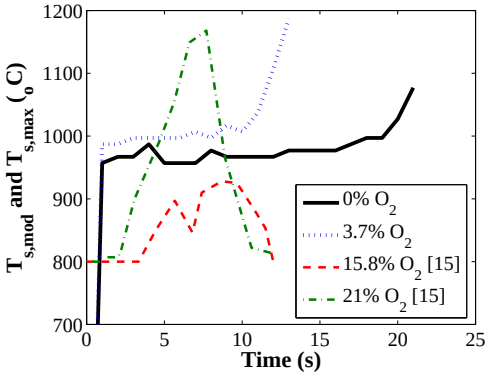
1200
1100
1000
900
800
700
0
5
10
15
20
25
Time (s)
T s,mod and T s,max (°C)
0% O2
3.7% O2
15.8% O2 [15]
21% O2 [15]

Figure 9

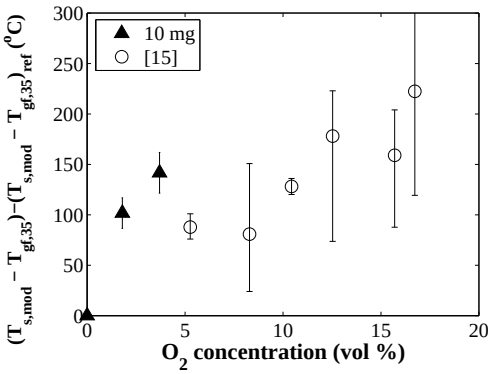
10 mg
[15]
$(T_{s,mod} - T_{gf,35}) - (T_{s,mod} - T_{gf,35})_{ref}$ (°C)
O_2 concentration (vol %)
0
50
100
150
200
250
300
0
5
10
15
20

Figure 10

Chapter 5

Influence of Droplet Size on the Release of Atomic Sodium from a Burning Black Liquor Droplet in a Flat Flame

W.L. Saw [a,b], G.J. Nathan [a,b], P.J. Ashman [a,c], and M. Hupa [d]

[a]Centre for Energy Technology, The University of Adelaide, SA 5005 Australia

[b]School of Mechanical Engineering, The University of Adelaide, SA 5005 Australia

[c]School of Chemical Engineering, The University of Adelaide, SA 5005 Australia

[d]Process Chemistry Centre, Åbo Akademi Biskopsgatan 8, FI-20500 Åbo, Finland

Submitted to Fuel on 5th June 2009

Statement of Authorship

Influence of Droplet Size on the Release of Atomic Sodium from a Burning Black Liquor Droplet in a Flat Flame

Submitted to Fuel on 5th June 2009

SAW, W.L. (Candidate)

I performed the measurements and data processing, wrote the first draft of the manuscript and incorporated and addressed all comments and suggestions by other authors in subsequent revisions of the manuscript. Interpretation of the data was my responsibility.

I hereby certify that the statement of contribution is accurate

Signed Date

NATHAN, G.J.

I was principal supervisor for the development of work, contributed to both data interpretation and refining of the manuscript.

I hereby certify that the statement of contribution is accurate and I have given written permission for this paper to be included in this thesis.

Signed _____ Date_____

ASHMAN, P.J.

I jointly contributed to both data interpretation and refining of the manuscript.

I hereby certify that the statement of contribution is accurate and I have given written permission for this paper to be included in this thesis.

Signed _____ Date_____

HUPA, M.

I jointly contributed to data interpretation.

I hereby certify that the statement of contribution is accurate and I have given written permission for this paper to be included in this thesis.

Signed _____ Date_____

Saw, W.L., Nathan, G.J., Ashman, P.J. & Hupa, M. (2010) Influence of droplet size on the release of atomic sodium from a burning black liquor droplet in a flat flame. *Fuel, v. 89(8), pp. 1840-1848*

Chapter 6

The Influence of Boron on the Emission of Sodium During Burning Black Liquor Combustion Under Oxidative Conditions

W.L. Saw [a], M. Forssén [b], M. Hupa [b], G.J. Nathan [a], and P.J. Ashman [c]

[a]Centre for Energy Technology, School of Mechanical Engineering, The University of Adelaide, SA 5005 Australia

[b]Process Chemistry Centre, Åbo Akademi Biskopsgatan 8, FI-20500 Åbo, Finland

[c]Centre for Energy Technology, School of Chemical Engineering, The University of Adelaide, SA 5005 Australia

Appita J. 62 (2009) 219–225

Statement of Authorship

The Influence of Boron on the Emission of Sodium During Burning Black Liquor Combustion Under Oxidative Conditions

***Appita J.* 62 (2009) 219–225**

SAW, W.L. (Candidate)

I performed the measurements and data processing under the supervision of Mikael Forssén. I wrote the first draft of the manuscript and incorporated and addressed all comments and suggestions by other co-authors in subsequent revisions of the manuscript. Interpretation of the data was my responsibility.

I hereby certify that the statement of contribution is accurate

Signed Date

FORSSÉN, M.

I supervised the development of work, jointly contributed to both data interpretation and refining of the manuscript.

I hereby certify that the statement of contribution is accurate and I have given written permission for this paper to be included in this thesis.

Signed _____ Date_____

HUPA, M.

I jointly contributed to both data interpretation and refining of the manuscript.

I hereby certify that the statement of contribution is accurate and I have given written permission for this paper to be included in this thesis.

Signed _____ Date_____

NATHAN, G.J.

I jointly contributed to both data interpretation and refining of the manuscript.

I hereby certify that the statement of contribution is accurate and I have given written permission for this paper to be included in this thesis.

Signed _____ Date_____

ASHMAN, P.J.

I jointly contributed to refining of the manuscript.

I hereby certify that the statement of contribution is accurate and I have given written permission for this paper to be included in this thesis.

Signed _____ Date_____

Saw, W.L., Forssen, M., Hupa, M. Nathan, G.J., Ashman, P.J. & (2009) The influence of boron on the emission of sodium during black liquor combustion under oxidative conditions.
Appita Journal, v. 62(3), pp. 219-225

NOTE:
This publication is included on pages 119-125 in the print copy of the thesis held in the University of Adelaide Library.

Chapter 7

Influence of Stoichiometry on the Release of Atomic Sodium from a Burning Black Liquor Droplet in a Flat Flame With and Without Boron

W.L. Saw [a,b], M. Hupa [c], G.J. Nathan [a,b], and P.J. Ashman [a,d]

[a]Centre for Energy Technology, The University of Adelaide, SA 5005 Australia

[b]School of Mechanical Engineering, The University of Adelaide, SA 5005 Australia

[c]Process Chemistry Centre, Åbo Akademi Biskopsgatan 8, FI-20500 Åbo, Finland

[d]School of Chemical Engineering, The University of Adelaide, SA 5005 Australia

Fuel, 10.1016/j.fuel.2009.11.023

Statement of Authorship

Influence of Stoichiometry on the Release of Atomic Sodium from a Burning Black Liquor Droplet in a Flat Flame With and Without Boron

Fuel, 10.1016/j.fuel.2009.11.023

SAW, W.L. (Candidate)

I performed the measurements and data processing. I wrote the first draft of the manuscript and incorporated and addressed all comments and suggestions by other authors in subsequent revisions of the manuscript. Interpretation of the data was my responsibility.

I hereby certify that the statement of contribution is accurate.

Signed Date

HUPA, M.

I jointly contributed to both data interpretation and refining of the manuscript.

I hereby certify that the statement of contribution is accurate and I have given written permission for this paper to be included in this thesis.

Signed _____ Date_____

NATHAN, G.J.

I was principal supervisor for the development of work, contributed to both data interpretation and refining of the manuscript.

I hereby certify that the statement of contribution is accurate and I have given written permission for this paper to be included in this thesis.

Signed _____ Date_____

ASHMAN, P.J.

I jointly contributed to both data interpretation and refining of the manuscript.

I hereby certify that the statement of contribution is accurate and I have given written permission for this paper to be included in this thesis.

Signed _____ Date_____

Saw, W.L., Hupa, M., Nathan, G.J. & Ashman, P.J. (2010) Influence of stoichiometry on the release of atomic sodium from a burning black liquor droplet in a flat flame with and without boron.
Fuel, v. 89(9), pp. 2608-2616

Chapter 8

Conclusion

"It does not matter how slowly you go
as long as you do not stop."

Confucius

The use of a simultaneous PLIF and absorption technique to measure the temporal history and the release rate of sodium from a burning black liquor droplet in a flat flame under reducing and oxidising conditions has been successfully demonstrated for the first time. The development of this simultaneous technique with an iterative correction method could also be applied to measure other inorganic species at high concentration. The highest concentration of atomic sodium was measured in the final stage of black liquor combustion - that of smelt coalescence, where the concentration is an order of magnitude greater than in the other stages combined. While the extensive release of atomic sodium from this final combustion stage applies to only a relatively small percentage of the mass of black liquor in a kraft recovery boiler, the effect could still be significant in fume formation. This is because the extensive release is expected to occur only in the very small droplets, predominantly generated by splitting or physical ejection, which, while small in mass, are large in number. Small droplets have a very short combustion time and so could remain in suspension within hot gases for sufficient time for extensive release of their sodium.

The gaseous environment of the present flat flame burner is different from that examined previously within closed furnaces to study the loss of sodium during combustion of black liquor. However, the flat flame burner has improved optical access for the PLIF technique over a closed furnace. Furthermore, particle temperatures similar to those in furnaces can be achieved, and the gaseous environment can be controlled. Importantly, no physical ejection was detected during any of the stages of combustion in the present flame. The lack of ejecta was further evidenced by the analysis of sodium left in the residue. The ability to avoid physical ejection has scientific advantages, since it allows the combustion and ejection processes to be isolated.

The temporal history and the release rates of atomic sodium from a burning black liquor droplet, especially during the smelt coalescence stage are strongly dependent on equivalence ratio (or excess oxygen). The concentration of atomic sodium in the plume under reducing conditions was found to be higher than that under oxidising conditions by at least a factor of 2.5, and the signal was found to be constant during the smelt coalescence stage. Interestingly, three phases of smelt coalescence were identified under oxidising conditions with a peak in each phase. This was not known previously, since this information cannot be obtained based on an analysis of the sodium in the residue. The release rate of atomic sodium increases parabolically as the initial droplet size is decreased for all the stages of black liquor combustion. This shows that significant fume formation can occur during the in-flight combustion of the carryover or the ejecta.

Given that only 0.37% of boron added by weight, some significant influences in the present flat flame environment were found during combustion, especially during the smelt coalescence stage. A small and repeatable increase in the drying and devolatilisation times was also observed at low oxygen concentrations in the flat flame environment, which was found to be relatively similar to that within a closed furnace. However, the influences appear complex and more work is required to understand them better. The addition of boron to the liquor clearly reduced the total atomic sodium released during the char consumption stage by 120% and 180% at 1.8% and 3.7% $O_{2,\,bg}$, respectively. On the other hand, the most significant influence of boron on the loss of sodium from black liquor combustion within the closed furnace was found to occur during the smelt oxidation stage. This decrease in atomic sodium released and its release rate may have major practical significance and requires more work.

The statistical distribution of surface temperature has also been assessed for the first time for a black liquor droplet using two-dimensional two-colour optical pyrometry. The influence of distribution of surface temperature, together with the change in the external surface area of the droplet on the release of atomic sodium has also been successfully assessed simultaneously. The gas flame temperature in the present environment, however, is higher than that within a closed furnace or a kraft recovery boiler by approximately 500ºC. Nonetheless, the measured surface temperature of a burning droplet in the flat flame was found to be relatively similar to that within the closed furnace.

The release of atomic sodium during the initial three stages of combustion was found to be insignificant both by the PLIF technique, and by the total loss of sodium, which was based on the analysis of the residue from black liquor combustion in the flat flame. The present flame inhibits the release of atomic sodium or total sodium and eliminates physical ejection. These new measurements provide new insight into the temporal history and the release rate of atomic sodium, which can be used to support the development of sub-models for CFD models in order to better understand and optimise fume formation in a kraft recovery boiler or in a gasifier. Hence, the issues of unscheduled shutdown of a pulp and paper mill caused by fouling and corrosion to the heat exchanger tubes in the upper furnace of a recovery boiler can potentially be minimised.

Further investigations could be usefully performed to measure the temporal release of atomic sodium under different oxidising environment by replacing the present fuel, natural gas, with other types of fuel, such as H_2 or CO to study the effects of H_2O and CO_2 individually. This laser diagnostic technique could also be applicable to a special design SDF with suitable optical access for lasers and ICCD cameras.